



HAL
open science

The impact of gut microbiota on depressive-like behaviors and adult hippocampal neurogenesis requires the endocannabinoid system

Grégoire Chevalier, Eleni Siopi, Laure Guenin-Macé, Maud Pascal, Thomas Laval, Aline Rifflet, Ivo Gomperts Boneca, Caroline Demangel, François Leulier, Gabriel Lepousez, et al.

► To cite this version:

Grégoire Chevalier, Eleni Siopi, Laure Guenin-Macé, Maud Pascal, Thomas Laval, et al.. The impact of gut microbiota on depressive-like behaviors and adult hippocampal neurogenesis requires the endocannabinoid system. 2021. pasteur-02873657

HAL Id: pasteur-02873657

<https://pasteur.hal.science/pasteur-02873657>

Preprint submitted on 11 Jun 2021

HAL is a multi-disciplinary open access archive for the deposit and dissemination of scientific research documents, whether they are published or not. The documents may come from teaching and research institutions in France or abroad, or from public or private research centers.

L'archive ouverte pluridisciplinaire **HAL**, est destinée au dépôt et à la diffusion de documents scientifiques de niveau recherche, publiés ou non, émanant des établissements d'enseignement et de recherche français ou étrangers, des laboratoires publics ou privés.



Distributed under a Creative Commons Attribution - NonCommercial - NoDerivatives 4.0 International License

1
2
3
4
5
6
7
8
9
10
11
12
13
14
15
16
17
18
19
20
21
22
23

The impact of gut microbiota on depressive-like behaviors and adult hippocampal neurogenesis requires the endocannabinoid system

Grégoire Chevalier¹, Eleni Siopi^{2,#}, Laure Guenin-Macé^{3,#}, Maud Pascal^{1,2,#}, Thomas Laval³, Aline Rifflet⁴, Ivo Gomperts Boneca⁴, Caroline Demangel³, François Leulier⁵, Gabriel Lepousez^{2,†}, Gérard Eberl^{1,†,*} & Pierre-Marie Lledo^{2,†,*}

¹ Microenvironment and Immunity Unit, Institut Pasteur, INSERM U1224, Paris, France

² Perception and Memory Unit, Institut Pasteur, CNRS UMR3571, Paris, France

³ Immunobiology of Infection Unit, Institut Pasteur, INSERM U1221, Paris, France

⁴ Biology and Genetics of Bacterial Cell Wall Unit, Institut Pasteur, Paris, France

⁵ Institut de Génomique Fonctionnelle de Lyon, Université de Lyon, Ecole Normale Supérieure de Lyon, CNRS UMR 5242, Lyon, France

Contributed equally

† Contributed equally

* Corresponding authors: pierre-marie.lledo@pasteur.fr and gerard.eberl@pasteur.fr

24 **SUMMARY**

25 Depression is the leading cause of disability worldwide. Recent observations have
26 revealed an association between mood disorders and alterations of the intestinal
27 microbiota, but causality remains yet to be established. Here, using unpredictable
28 chronic mild stress (UCMS) as a mouse model of depression, we show that the UCMS
29 mice display phenotypic alterations — characterized by an altered gut microbiota
30 composition, a reduced adult hippocampal neurogenesis and a depressive-like
31 behaviors — which could be transferred from UCMS donors to naïve recipient mice by
32 fecal microbiota transplantation. The cellular and behavioral alterations observed in
33 recipient mice were accompanied by a decrease in the endocannabinoid (eCB)
34 signaling due to lower peripheral levels of fatty acid precursors of eCB ligands. The
35 adverse effects of UCMS-transferred microbiota on adult neurogenesis and behavior
36 in naïve recipient mice were alleviated by selectively enhancing the central eCB tone
37 or by adding arachidonic acid, a fatty acid precursor of eCB ligands, to the diet. In the
38 gut of both UCMS donors and recipients, the microbiota composition was
39 characterized by a relative decrease in *Lactobacilli* abundance, and complementation
40 of the UCMS recipient microbiota with a strain of the *Lactobacilli* genus was sufficient
41 to restore normal eCB brain levels, hippocampal neurogenesis and to alleviate
42 depressive-like behaviors. Our findings provide a mechanistic scenario for how chronic
43 stress, diet and gut microbiota dysbiosis generate a pathological feed-forward loop that
44 contributes to despair behavior via the central eCB system.

45 INTRODUCTION

46 Depression is the leading cause of disability worldwide, currently affecting more than
47 300 million people¹. Despite the prevalence of depression and its considerable
48 economic impact, its pathophysiology remains highly debated. Yet, a better
49 understanding of the mechanisms leading to depression is a prerequisite for
50 developing efficient therapeutic strategies. However, unraveling the pathophysiology
51 of depression is challenging, as depressive syndromes are heterogeneous and their
52 etiologies likely to be diverse. Experimental and genetic studies have yielded several
53 mechanisms including maladaptive responses to stress with HPA axis dysregulation,
54 inflammation, reduced neuroplasticity, circuit dysfunctions and perturbation in
55 neuromodulatory systems such as monoaminergic and endocannabinoid (eCB)
56 systems.

57 A number of studies converge to indicate hippocampal alterations as critical in
58 the pathogenesis of depression. For instance, hippocampal volume loss is a hallmark
59 of clinical depression²⁻⁴. Likewise, rodent studies have demonstrated that chronic
60 stress-induced depression impair adult hippocampal neurogenesis⁵⁻⁸. Furthermore,
61 impaired hippocampal neurogenesis results in depressive-like behaviors in rodent, in
62 part because hippocampal neurogenesis buffers the over-reactivity of the
63 hypothalamic-pituitary-adrenal (HPA) axis in response to stress⁹⁻¹¹. In that line,
64 antidepressants and alternative antidepressant interventions stimulate adult
65 hippocampal neurogenesis, which in turn dampens stress responses and restores
66 normal behavior¹²⁻¹⁴. Adult hippocampal neurogenesis is thus considered as an
67 important causal factor and a key marker of depression, although a direct causal link
68 is still missing in human depression^{15,16}.

69

70 Over the last decade, the impact of the symbiotic microbiota on numerous host
71 functions has been increasingly recognized. The wide variety of intestinal microbes
72 affects many processes including immunity¹⁷, metabolism¹⁸ and the central nervous
73 system¹⁹. In depressed patients, alterations in the composition of the intestinal
74 microbiota (named dysbiosis) have been characterized^{20,21}. Furthermore, numerous
75 studies on animal models have shown that the microbiota modulates anxiety²²⁻²⁴ and
76 onset of neurological diseases associated to circuit dysfunctions^{25,26} by releasing
77 bacterial metabolites that can directly or indirectly affect brain homeostasis^{19,27}. In that
78 line of ideas, microbiota from depressed patients alter behavior when transferred to
79 antibiotic-treated rats²⁸ and murine gut microbiota dysbiosis is associated with several
80 neurobiological features of depression, such as low-grade chronic inflammation²⁹,
81 abnormal activity of the HPA axis^{30,31} and decreased adult neurogenesis^{12,32}. The
82 notion that microbiota is a critical node in the gut-brain axis is also supported by the
83 observation that colitis, which depends on the gut microbiota, shows significant
84 comorbidities with depression³³. Finally, probiotic intervention has been shown to
85 influence emotional behavior in animal models of depression³⁴⁻³⁶ and improve mood
86 in depressive patients³⁷⁻³⁹. However, the molecular mechanisms linking intestinal
87 microbiota and mood disorders remain largely unknown, partly due to the lack of
88 experimental models.

89 To explore a causative role of the gut microbiota in stress-induced depressive
90 behaviors, we used unpredictable chronic mild stress (UCMS), a mouse model of
91 depression, and fecal microbiota transfer (FMT) from stressed donors to naïve mice.
92 We found that the microbiota transplantation transmits the depressive behavioral
93 symptoms, and reduces adult neurogenesis of the recipient mice. Metabolomic
94 analysis reveals that recipient mice developed an altered fatty acid metabolism

95 characterized by deficits in lipid precursors for eCBs, which resulted in impaired activity
96 of the eCB system in the brain. Increase of the eCB levels after pharmacological
97 blocking of the eCB degrading enzymes, or complementation of the diet with
98 arachidonic acid, a precursor of eCBs, is sufficient to normalize both the microbiota-
99 induced depressive-like behaviors and hippocampal neurogenesis in recipient mice.
100 Lastly, our study reveals that UCMS induced a gut microbiota dysbiosis characterized
101 by a decrease in *Lactobacilli* abundance also observed in recipient mice.
102 Complementation of recipient mice with a strain of the *Lactobacilli* genus is sufficient
103 to restore both eCB brain levels and hippocampal neurogenesis, alleviating the
104 microbiota-induced despair behavior.

105 **RESULTS**

106

107 **Transplantation of microbiota from stressed mice to naïve recipients transfers** 108 **depressive-like behaviors and reduces adult neurogenesis**

109 To establish a depressive-like state in mice, we submitted C57BL/6J mice for 8 weeks
110 to UCMS, a well-defined mouse model of stress-induced depression^{40–42} (**Fig. 1A** and
111 **Supplementary Table S1**). Consistent with previous reports, UCMS mice developed
112 depressive-like behaviors, as shown by increased feeding latency in the “novelty
113 suppressed feeding test” as compared to control mice (**Fig. 1B**), even though feeding
114 drive was not affected (**Supplementary Fig. 1A**). This behavior reflects both anxiety
115 and anhedonia. However, UCMS mice did not develop increased anxiety, as
116 determined by the “light/dark box test” (**Fig. 1C**). Furthermore, UCMS mice showed
117 increased grooming latency (**Fig. 1D**) and decreased self-grooming behavior in the
118 “splash test” (**Supplementary Fig.1B and C**), reflecting symptoms of depression such
119 as apathetic behavior⁴¹. The depressive-like state seen in UCMS mice was further
120 confirmed in two prototypical tests for assessing depressive-like behaviors, the “tail
121 suspension test” and the “forced swim test” (also named behavioral despair tests).
122 UCMS mice showed increased immobility time in these two tests compared to control
123 mice (**Fig. 1E and F**). We also observed that UCMS mice gained significantly less
124 weight over time than control mice, as previously reported⁴³ (**Supplementary Fig. 1D**).
125 Altogether, these different behavioral tests demonstrate that 8 weeks of UCMS induce
126 depressive-like but not anxiety-like behaviors in C57BL/6 mice.

127 As the reduction of adult hippocampal neurogenesis is a hallmark of depression,
128 we tested whether UCMS affected the number of adult-born neurons in the dentate
129 gyrus (DG) of the hippocampus. The decreased number of proliferating neural stem

130 cells labeled with the cell proliferation marker Ki67 (**Fig. 1G** and **H**), and of doublecortin
131 (DCX)⁺ cells, a marker for newborn immature neurons (**Fig. 1G** and **I**), shows that
132 UCMS mice exhibit reduced hippocampal neurogenesis.

133 We next assessed whether the transplantation of gut microbiota from UCMS
134 mice to naïve unstressed hosts was sufficient to transfer the hallmarks of depressive-
135 like state. To this end, we transferred the fecal microbiota of control or stressed mice
136 to adult germ-free mice (**Fig. 1A**). Eight weeks after FMT, recipients of UCMS
137 microbiota showed depressive-like behaviors in both the tail suspension and the forced
138 swim tests (**Fig. 1E** and **F**), which were confirmed in the splash test (**Fig. 1D** and
139 **Supplementary Fig. 1F** and **G**) and the novelty suppressed feeding test (**Fig. 1B** and
140 **Supplementary Fig. 1E**). As in UCMS donors, recipient mice did not express anxiety-
141 related behaviors (**Fig. 1C**). Similar results were obtained when UCMS microbiota was
142 transferred to recipient SPF mice that were treated with broad-spectrum antibiotics for
143 6 days until one day prior to FMT (**Supplementary Fig. 2**). Because germ-free mice
144 might exhibit some behavioral abnormalities due to sustained disruption in the
145 microbiota-gut-brain axis, all subsequent experiments were performed using short-
146 term antibiotic-treated recipient mice. Finally, recipients of UCMS microbiota also
147 showed decreased proliferation of neural stem cells (**Fig. 1G** and **H**) and decreased
148 production of new neurons in the hippocampus (**Fig. 1G** and **I**). These data
149 demonstrate that the hallmarks of depressive-like behaviors are transferable to naïve
150 recipient mice by the transplantation of fecal microbiota obtained from stressed-
151 induced depressive mice.

152 **Gut microbiota from stressed mice alters fatty acid metabolism and the**
153 **hippocampal endocannabinoid system**

154 We explored the possibility that UCMS microbiota triggered depressive-like behaviors
155 through alterations of the host's metabolism. Metabolomic profiling of serum revealed
156 a significant decrease in the levels of monoacylglycerols (MAG) and diacylglycerols
157 (DAG) in both UCMS mice and recipients of UCMS microbiota, as compared to control
158 and recipients of control microbiota (**Fig. 2A**). Furthermore, the n-6 polyunsaturated
159 fatty acid (PUFA), arachidonic acid (AA, 20:4n-6), its precursor linoleic acid (18:2n-6),
160 and n6-PUFA biosynthesis intermediates, were significantly decreased in both UCMS
161 donors and recipients (**Fig. 2B and C**). This lipids loss was specific to short-chain fatty
162 acids since levels of several medium- and long-chain fatty acylcarnitines rather
163 increased in UCMS microbiota recipients (**Supplementary Fig. 3**).

164 Such changes in the levels of fatty acids could originate from altered gut
165 permeability and/or dysbiosis-induced lipid metabolism changes. To test the first
166 hypothesis, we quantified fluorescence level in the serum following gavage with FITC-
167 dextran and found no change in gut permeability (**Supplementary Fig. 3E**). To
168 address the second hypothesis, we scrutinize several fatty acid metabolites and found
169 that two precursors for the production of eCB, AA-containing DAG and n-6 PUFA, were
170 dramatically reduced in recipient mice transplanted with UCMS microbiota but not with
171 control microbiota. Interestingly, dysregulation of the eCB system and its main central
172 receptor CB1 has been associated with the pathophysiology of depression both in
173 humans and in UCMS model of depression^{44,45}.

174 Since previous studies have shown that activation of the CB1 receptors
175 produces anxiolytic and antidepressant-like effects, notably via the modulation of
176 hippocampal neurogenesis⁴⁶⁻⁴⁸, we investigated into more details the brain eCB

177 system. We examined both the hippocampal production of eCB ligands and the
178 activation level of the CB1 receptor pathway. As the AA-containing DAG and n-6 PUFA
179 are precursors of the endocannabinoid 2-arachidonoylglycerol (2-AG), we first
180 compared the levels of 2-AG and its more stable metabolite 1-AG in the hippocampus
181 and serum of donor and recipient mice⁴⁹. Levels of hippocampal 2-AG, determined by
182 mass spectrometry, revealed a significant decrease in both UCMS donors and
183 recipients (**Fig. 2D**), with a strong inverse correlation found between the serum levels
184 of 1-AG and the depressive state (**Fig. 2E**). Similar results were reported for other
185 eCBs (**Fig. 2F**).

186 In the hippocampus, activation of CB1 receptors triggers mTOR signaling. To
187 evaluate whether deficiency in 2-AG leads to altered activity of the mTOR pathway, we
188 quantified phosphorylated (active) mTOR and its downstream effectors in both UCMS
189 donor and recipient mice. mTOR phosphorylates the 70-kDa ribosomal protein S6
190 kinase (p70S6K) at T389⁵⁰ and the activated p70S6K in turn phosphorylates the
191 ribosomal protein S6 (rpS6) at S235/236, which initiates mRNA translation⁵¹. Donors
192 and recipients of UCMS microbiota showed significantly decreased phosphorylation of
193 mTOR (p-mTOR), p70S6K (p-p70S6K), and rpS6 (p-rpS6) (**Fig. 2G to I**). Collectively,
194 these results demonstrate that the signature in lipid metabolism of UCMS microbiota
195 comprises a deficiency in serum 2-AG precursors, lower content in hippocampal 2-AG
196 and breakdown of the mTOR signaling. Remarkably, these features were found to be
197 transmittable to naïve recipient mice following FMT.

198

199 **Restoration of eCB signaling normalizes behavior and adult neurogenesis**

200 To further demonstrate the role of defective eCB signaling in the depressive-like
201 behaviors of mice transferred with UCMS microbiota, we next assessed whether

202 enhancing eCB signaling, using pharmacological blockade of the 2-AG-degrading
203 enzyme monoacylglycerol lipase (MAGL), could alleviate these phenotypes.
204 Recipients of UCMS microbiota were treated with the MAGL inhibitor JZL184, or
205 JZL184 together with rimonabant, a selective antagonist of CB1, every 2 days for 4
206 weeks starting 4 weeks after FMT (**Fig. 3A**). First, we confirmed that recipients of
207 UCMS microbiota treated with JZL184 showed a significant increase in hippocampal
208 levels of p-mTOR, p-p70S6K, and p-rpS6 as compared to vehicle-treated recipient
209 mice of UCMS microbiota (**Fig. 3B** and **C**). Furthermore, consistent with enhanced
210 eCB signaling, we confirmed that JZL184 enhanced the levels of 2-AG in the
211 hippocampus (**Fig. 3D**)^{52,53}. The effect of JZL184 was strictly CB1-dependent as it was
212 reversed by the selective CB1 receptor antagonist rimonabant. As a consequence,
213 JZL184 reduced depressive symptoms in recipients of UCMS microbiota, an effect that
214 was blocked by rimonabant (**Fig. 3E to H**). To assess the relative contribution of central
215 *versus* peripheral CB1 receptors in these depressive-like behaviors, we compare the
216 effects of rimonabant to the effects of AM6545, a CB1 antagonist with limited brain
217 penetrance⁵⁴. In contrast to rimonabant, AM6545 did not reverse the antidepressant
218 effect of JZL184 (**Fig. 3G** and **H**), indicating that central CB1 signaling is necessary to
219 alleviate depressive-like behaviors, at least in our model.

220 JZL184 also alleviates the detrimental effects of UCMS microbiota on adult
221 hippocampal neurogenesis. JZL184 treatment rescued the proliferation and
222 differentiation of neural stem cells in the hippocampus of UCMS microbiota recipients,
223 an effect that was blocked by rimonabant (**Fig. 4A, B**). The survival of newly-generated
224 neurons was also increased in the hippocampus of mice treated with JZL184, and
225 blocked by rimonabant, as shown by the quantification of newborn neurons labeled
226 with the DNA synthesis marker EdU administered 4 weeks before analysis (**Fig. 4C**).

227 According to the regions of the hippocampus, adult neurogenesis may subserve
228 different functions: new neurons born in the dorsal hippocampus influences
229 cognitive information processing whereas adult-born neurons of the ventral
230 hippocampus regulate mood and stress response⁵⁵. In the present study, the effects
231 on UCMS microbiota on adult hippocampal neurogenesis were observed both in the
232 dorsal and ventral regions of the hippocampus (**Suppl. Fig 4**). Together, these data
233 demonstrate that the decrease in hippocampal neurogenesis and depressive-like
234 behaviors observed in recipients of UCMS microbiota can be rescued by selectively
235 increasing the activity of the brain eCB system.

236 We next reasoned that if UCMS microbiota induces paucity in serum levels of
237 eCB precursors, the complementation of diet with eCB precursors, such as arachidonic
238 acid (AA) might normalize the levels of 2-AG and restore normal behavior. Recipient
239 mice of UCMS microbiota were given orally AA during 5 weeks starting 3 weeks after
240 microbiota transfer (**Fig. 5A**). Remarkably, we observed that AA treatment restored
241 normal levels of hippocampal 2-AG (**Fig. 5B**) and reversed the depressive-like
242 behaviors induced by UCMS microbiota (**Fig. 5C** and **D**). Furthermore, AA
243 complementation also partially restored the production and the survival of hippocampal
244 newborn neurons (**Fig. 5E** and **F**).

245

246 **UCMS-induced dysbiosis and complementation with *Lactobacillus plantarum*^{WJL}**

247 We next investigated how UCMS affected the composition of the microbiota that was
248 responsible for the observed cellular and behavioral impairments in recipient mice. The
249 composition of the fecal microbiota was determined by sequencing of 16S rDNA.
250 Analysis of bacterial families revealed significant modifications in the microbiota of
251 UCMS mice, as compared to the microbiota of control mice raised in separate cages

252 **(Fig. 5G)**, while the total number of species (alpha diversity) did not vary significantly
253 **(Fig. 5H)**. In-depth analysis of bacterial families showed an increase in
254 *Ruminococcaceae*, and *Porphyromonadaceae*, as well as a decrease in
255 *Lactobacillaceae* in UCMS mice **(Fig. 5G and Supplementary Fig. 5)**. These results
256 are in agreement with recent studies reporting an association between low frequencies
257 of *Lactobacilli* and stress in mice^{56–58} or depression in patients⁵⁹. Importantly, the
258 differences in microbiota composition between recipient mice of UCMS and control
259 microbiota were maintained 8 weeks after transfer **(Fig. 5G)**, in particular the decrease
260 in *Lactobacillaceae* **(Fig. 5G and Supplementary Fig. 5)**, while the total number of
261 species (alpha diversity) did not vary **(Fig. 5H)**.

262 Since the frequencies of *Lactobacillaceae* were decreased in UCMS microbiota
263 when compared to control microbiota **(Fig. 5G)**, we tested whether complementation
264 of UCMS microbiota with *Lactobacillaceae* normalized behaviors and neurogenesis
265 levels in recipients of UCMS microbiota. To this end, the microbiota of recipients was
266 complemented with a strain of *Lactobacillus plantarum* (*Lp^{WJL}*) shown to modulate the
267 host's lipid composition^{60,61}, to stimulate juvenile growth⁶² and to influence affective
268 behavior in mice⁶³. Recipient mice of UCMS microbiota were given orally *Lp^{WJL}* for 5
269 weeks starting 3 weeks after microbiota transfer **(Fig. 5A)**. We observed that *Lp^{WJL}*
270 restored normal levels of hippocampal 2-AG **(Fig. 5B)**, reversed the depressive-like
271 behaviors induced by UCMS microbiota **(Fig. 5C and D)** and partially restored the
272 production and the survival of hippocampal newborn neurons **(Fig. 5E and F)**. These
273 data indicate that *Lactobacillaceae* play an important role in the host metabolism with
274 significant effect on mood control.

275 **DISCUSSION**

276 In the present study, we have explored the mechanisms by which gut microbiota
277 dysbiosis contributes to brain dysfunctions and behavioral abnormalities associated
278 with depressive-like states. Chronic stress is recognized as a major risk factor for
279 depression⁶⁴ and most animal models of depressive-like behaviors rely on chronic
280 stress or manipulation of the stress-sensitive brain circuits⁶⁵. Using UCMS as a mouse
281 model of depression, we showed that, upon transplantation to naïve hosts, the
282 microbiota from UCMS mice reduced adult hippocampal neurogenesis and induced
283 depressive-like behaviors.

284 Searching for mechanistic explanations of these dysfunctions, we found that
285 UCMS microbiota alters the fatty acid metabolism of the host, leading to paucity in
286 precursors of the eCB system, such as AA, reduced production of the eCB 2-AG in the
287 hippocampus, and diminished signaling in the hippocampal eCB system. Restoration
288 of normal eCB signaling levels in mice recipient of UCMS microbiota after blocking the
289 2-AG-degrading enzyme, or after complementation of the diet with the 2-AG precursor
290 AA, both restored adult neurogenesis and behaviors. Finally, UCMS-induced
291 perturbations of the gut bacterial composition were characterized by loss of
292 *Lactobacillaceae*, an alteration that was maintained after microbiota transplantation to
293 naïve hosts. The mere complementation of the UCMS recipients' microbiota with
294 *Lactobacillus plantarum* Lp^{WJL} was sufficient to normalize the levels of 2-AG in the
295 hippocampus and restore affective behaviors and adult hippocampal neurogenesis.

296 The eCB system has been reported to regulate mood, emotions and responses
297 to stress through activation of the cannabinoid receptor CB1. For instance, the CB1
298 receptor antagonist rimonabant, initially prescribed for the treatment of obesity and
299 associated metabolic disorders, increases the incidence of depressive symptoms⁶⁶.

300 Furthermore, a higher frequency in a mutant allele for the CB1 receptor gene *CNR1* is
301 observed in depressed patients⁶⁷. In contrast, cannabis (that includes the eCB ligand
302 delta-9 tetrahydrocannabinol or THC) improves mood in humans⁶⁸ and synthetic CB1
303 agonists produce anxiolytic- and antidepressant-like effects in animal models⁶⁹. In
304 particular, chronic stress has been showed to decrease eCB signaling in the brain⁷⁰⁻
305 ⁷⁴. Here, we show that the intestinal microbiota is sufficient to initiate a pathological
306 feed-forward loop for depressive disorders by impairing the eCB system in the
307 hippocampus, a brain region strongly involved in the development of depressive
308 symptoms. Previous studies have shown that the reduction in hippocampal CB1
309 signaling, involving mTOR, induces depressive-like behaviors⁷⁵, and different studies
310 on postmortem brains of depressed patients have shown deficits in mTOR
311 signaling^{76,77}. In line with this, we observed a specific decrease in 2-AG, one of the two
312 major eCB ligands, in mice receiving UCMS-derived microbiota, but not medium- or
313 long-chain fatty acids. This result is reminiscent to clinical observations reporting low
314 serum levels of 2-AG in patients suffering from depression, post-traumatic stress
315 disorder or chronic stress, but not of the other main eCB ligand anandamide⁷⁸⁻⁸⁰.

316 The eCB system exerts its pleiotropic effects through multiples neuronal
317 processes including, but not limited to, adult hippocampal neurogenesis. The eCB
318 system is known to regulates adult neurogenesis via the CB1 receptor⁸¹ expressed by
319 neural progenitor cells^{46,48}. CB1-deficient mice show impaired neural progenitor
320 proliferation, self-renewal, and neurosphere generation⁴⁶ whereas CB1 receptor
321 agonists increase neurogenesis^{69,82,83}. In addition to this neurogenic effect occurring
322 in the hippocampus, other CB1 receptor-dependent processes might contribute to the
323 pathophysiology of our microbiota-induced depression. Further studies should be
324 conducted to test whether other brain targets of eCB signaling are equally affected by

325 microbiota dysbiosis.

326 It has been reported previously that the microbiota modulates the activity of the
327 eCB system in the gut^{84–87}. In the present study, we further demonstrate that the
328 dysbiotic gut microbiota from UCMS mice is sufficient to induce dysregulation of the
329 eCB system in the brain. We report that this dysregulation originates from a systemic
330 decrease in eCB precursors. Modifications in gut microbiota composition following
331 chronic stress has been extensively reported^{56,58,88–90}. In particular, low frequencies of
332 *Lactobacillaceae* are correlated with stress levels in mouse models^{56–58}. Dysbiosis of
333 the gut microbiota and low *Lactobacilli* frequency have also been detected in
334 depressed patients^{20,21,28,59}, and transplantation of the microbiota from these patients
335 into germ-free mice induces depressive- or anxiety-like behaviors in the recipients^{28,91}.
336 In line with these results, a probiotic treatment with *Lactobacilli* ameliorates depressive-
337 and anxiety-like behaviors in mice^{58,63}. Gut microbiota also modulates adult
338 neurogenesis^{92,93} and a *Lactobacillus* strain has been shown to promote the survival
339 of hippocampal neuronal progenitor⁹². Numerous studies have shown that *Lactobacilli*
340 treatment, as well as the administration of other probiotics, are beneficial in significantly
341 lowering depression and anxiety scores in patients^{94–100}. *L. plantarum* in particular was
342 recently shown to alleviate stress and anxiety¹⁰¹. Our study demonstrating the
343 beneficial effects of *L. plantarum*^{WJL} to complement a maladaptive microbiota adds to
344 several emerging evidence showing an antidepressant effects of probiotics in major
345 depression^{99,100}. We have found that one of the mechanisms by which *Lactobacilli*
346 promotes these effects is through regulation of the bioavailability of eCB precursors.

347 A major finding of our study is that recipients of UCMS microbiota developed an
348 altered fatty acid metabolism characterized by deficiency in MAG, DAG and fatty acids.
349 Serum levels of MAG, DAG and PUFAs were inversely correlated with the severity of

350 depressive-like behaviors. Further studies should clarify whether serum levels of fatty
351 acid could be considered as earlier biomarker for mood disorders. It has been reported
352 that nutritional n-3 PUFA deficiency abolishes eCB-mediated neuronal functions¹⁰²,
353 and conversely, that n-3 PUFA dietary supplementation reverses some aspects of
354 UCMS-induced depressive-like behaviors in mice^{102,103}. We may speculate that UCMS
355 microbiota promotes the degradation of PUFA or alters the absorption of these fatty
356 acids. The mechanisms by which gut microbiota modulates the host's fatty acid
357 metabolism has been partially investigated in several animal models. Microbiota
358 regulates intestinal absorption and metabolism of fatty acids in the zebrafish^{104,105}, and
359 in rodents, *Lactobacilli* species modulate lipid metabolism^{106,107}. Specifically,
360 *Lactobacillus plantarum* modulates the host's lipid composition by reducing the level
361 of serum triglycerides in the context of high fat diet^{60,108,109}. Furthermore, in humans,
362 *Lactobacillus plantarum* is associated with lower levels of cholesterol⁶¹. It is proposed
363 that *Lactobacillus plantarum* regulates fatty acid metabolism and modifies fatty acid
364 composition of the host¹⁰⁷.

365 In sum, our data show that microbiota dysbiosis induced by chronic stress
366 affects lipid metabolism and the generation of eCBs, leading to decreased signaling in
367 the eCB system and reduced adult neurogenesis in the hippocampus. This might be
368 the pathway, at least in part, that links microbiota dysbiosis to mood disorders, which
369 in turn, may affect the composition of the gut microbiota through physiological
370 adjustments and modulation of the immune system. Because we were able to interrupt
371 this pathological feed-forward loop by administering arachidonic acid or a
372 *Lactobacillus* probiotic strain, our study supports the concept that dietary or probiotic
373 interventions might be efficient weapons in the therapeutic arsenal to fight stress-
374 associated depressive syndromes.

375 **ACKNOWLEDGEMENTS**

376 We would like to thank all the members of the Eberl and Lledo lab, as well as members
377 of the Peduto lab for insightful discussions, and Pr. Peduto for access to the Apotome
378 microscope. A special thanks also to the members of the Pasteur Animal Facility who
379 were essential for this project, and in particular Marion Bérard, Martine Jacob, Thierry
380 Angelique and Eddie Maranghi. This work was supported by the Major Federating
381 Program “Microbes & Brain” of the Institut Pasteur, Agence Nationale de la Recherche
382 Grant ANR-16-CE15-0021-02-PG-Brain, and a grant from the Fédération pour la
383 Recherche sur le Cerveau (FRC). The Lledo’s lab is supported by Agence Nationale
384 de la Recherche Grants ANR-16-CE37-0010-ORUPS and ANR-15-NEUC-0004-02
385 “Circuit-OPL,” Laboratory for Excellence Programme “Revive” Grant ANR-10-LABX-
386 73, and the Life Insurance Company AG2R-La Mondiale.

387

388 **AUTHOR CONTRIBUTIONS**

389 G.C., G.E. and P.M.L. conceived the study; G.C. established the methodology; G.C.,
390 E.S., M.P., L.G.M., T.L. and A.R. performed the experiments; G.C. wrote the original
391 manuscript, which was edited by all authors; G.C., G.E., P.M.L., I.G.B. and G.L.
392 secured funds; G.E., P.M.L., I.G.B. and C.D. provided resources, and G.E., P.M.L.,
393 I.G.B. and C.D. supervised the project.

394

395 **COMPETING INTERESTS**

396 The authors declare having no conflict of interest.

397 **REFERENCES**

- 398 1. Kupfer, D. J., Frank, E. & Phillips, M. L. Major depressive disorder: new clinical,
399 neurobiological, and treatment perspectives. *Lancet* **379**, 1045–1055 (2012).
- 400 2. Sheline, Y. I., Wang, P. W., Gado, M. H., Csernansky, J. G. & Vannier, M. W.
401 Hippocampal atrophy in recurrent major depression. *Proc. Natl. Acad. Sci. U.*
402 *S. A.* (1996).
- 403 3. Campbell, S. & MacQueen, G. An update on regional brain volume differences
404 associated with mood disorders. *Current Opinion in Psychiatry* (2006).
405 doi:10.1097/01.yco.0000194371.47685.f2
- 406 4. Shen, Z. *et al.* Changes of grey matter volume in first-episode drug-naive adult
407 major depressive disorder patients with different age-onset. *NeuroImage Clin.*
408 (2016). doi:10.1016/j.nicl.2016.08.016
- 409 5. Cameron, H. A. & Gould, E. Adult neurogenesis is regulated by adrenal
410 steroids in the dentate gyrus. *Neuroscience* (1994). doi:10.1016/0306-
411 4522(94)90224-0
- 412 6. Sahay, A. & Hen, R. Adult hippocampal neurogenesis in depression. *Nat.*
413 *Neurosci.* (2007). doi:10.1038/nn1969
- 414 7. Schoenfeld, T. J. & Gould, E. Stress, stress hormones, and adult
415 neurogenesis. *Experimental Neurology* (2012).
416 doi:10.1016/j.expneurol.2011.01.008
- 417 8. Sheline, Y. I., Liston, C. & McEwen, B. S. Parsing the Hippocampus in
418 Depression: Chronic Stress, Hippocampal Volume, and Major Depressive
419 Disorder. *Biol. Psychiatry* (2019). doi:10.1016/j.biopsych.2019.01.011
- 420 9. Snyder, J. S., Soumier, A., Brewer, M., Pickel, J. & Cameron, H. A. Adult
421 hippocampal neurogenesis buffers stress responses and depressive
422 behaviour. *Nature* **476**, 458–61 (2011).
- 423 10. Glover, L. R., Schoenfeld, T. J., Karlsson, R. M., Bannerman, D. M. &
424 Cameron, H. A. Ongoing neurogenesis in the adult dentate gyrus mediates
425 behavioral responses to ambiguous threat cues. *PLoS Biol.* (2017).
426 doi:10.1371/journal.pbio.2001154
- 427 11. Egeland, M., Zunszain, P. A. & Pariante, C. M. Molecular mechanisms in the
428 regulation of adult neurogenesis during stress. *Nature Reviews Neuroscience*
429 (2015). doi:10.1038/nrn3855

- 430 12. Santarelli, L. *et al.* Requirement of Hippocampal Neurogenesis for the
431 Behavioral Effects of Antidepressants. *Science* (80-.). **301**, 805–809 (2003).
- 432 13. Surget, A. *et al.* Antidepressants recruit new neurons to improve stress
433 response regulation. *Mol. Psychiatry* (2011). doi:10.1038/mp.2011.48
- 434 14. Cullig, L. *et al.* Increasing adult hippocampal neurogenesis in mice after
435 exposure to unpredictable chronic mild stress may counteract some of the
436 effects of stress. *Neuropharmacology* (2017).
437 doi:10.1016/j.neuropharm.2017.09.009
- 438 15. Jacobs, B. L., Van Praag, H. & Gage, F. H. Adult brain neurogenesis and
439 psychiatry: A novel theory of depression. *Molecular Psychiatry* (2000).
440 doi:10.1038/sj.mp.4000712
- 441 16. Miller, B. R. & Hen, R. The current state of the neurogenic theory of depression
442 and anxiety. *Current Opinion in Neurobiology* (2015).
443 doi:10.1016/j.conb.2014.08.012
- 444 17. Belkaid, Y. & Hand, T. W. Role of the microbiota in immunity and inflammation.
445 *Cell* **157**, 121–41 (2014).
- 446 18. Cani, P. D. Metabolism in 2013: The gut microbiota manages host metabolism.
447 *Nat. Rev. Endocrinol.* **10**, 74–6 (2014).
- 448 19. Sharon, G. *et al.* The Central Nervous System and the Gut Microbiome. *Cell*
449 **167**, 915–932 (2016).
- 450 20. Jiang, H. *et al.* Altered fecal microbiota composition in patients with major
451 depressive disorder. *Brain. Behav. Immun.* **48**, 186–94 (2015).
- 452 21. Naseribafrouei, A. *et al.* Correlation between the human fecal microbiota and
453 depression. *Neurogastroenterol. Motil.* **26**, 1155–1162 (2014).
- 454 22. Bercik, P. *et al.* The intestinal microbiota affect central levels of brain-derived
455 neurotropic factor and behavior in mice. *Gastroenterology* **141**, 599–609,
456 609.e1–3 (2011).
- 457 23. Bravo, J. A. *et al.* Ingestion of Lactobacillus strain regulates emotional behavior
458 and central GABA receptor expression in a mouse via the vagus nerve. *Proc.*
459 *Natl. Acad. Sci. U. S. A.* **108**, 16050–5 (2011).
- 460 24. Heijtz, R. D. *et al.* Normal gut microbiota modulates brain development and
461 behavior. *Proc. Natl. Acad. Sci. U. S. A.* **108**, 3047–52 (2011).
- 462 25. Hsiao, E. Y. *et al.* Microbiota modulate behavioral and physiological
463 abnormalities associated with neurodevelopmental disorders. *Cell* **155**, 1451–

- 464 63 (2013).
- 465 26. Sampson, T. R. *et al.* Gut Microbiota Regulate Motor Deficits and
466 Neuroinflammation in a Model of Parkinson's Disease. *Cell* **167**, 1469-
467 1480.e12 (2016).
- 468 27. Schroeder, B. O. & Bäckhed, F. Signals from the gut microbiota to distant
469 organs in physiology and disease. *Nat. Med.* **22**, 1079–1089 (2016).
- 470 28. Kelly, J. R. *et al.* Transferring the blues: Depression-associated gut microbiota
471 induces neurobehavioural changes in the rat. *J. Psychiatr. Res.* **82**, 109–18
472 (2016).
- 473 29. Hodes, G. E., Kana, V., Menard, C., Merad, M. & Russo, S. J. Neuroimmune
474 mechanisms of depression. *Nat. Neurosci.* **18**, 1386–93 (2015).
- 475 30. Parker, K. J., Schatzberg, A. F. & Lyons, D. M. Neuroendocrine aspects of
476 hypercortisolism in major depression. *Horm. Behav.* **43**, 60–6 (2003).
- 477 31. McEwen, B. S. Physiology and neurobiology of stress and adaptation: central
478 role of the brain. *Physiol. Rev.* **87**, 873–904 (2007).
- 479 32. Sahay, A. & Hen, R. Adult hippocampal neurogenesis in depression. *Nat.*
480 *Neurosci.* **10**, 1110–1115 (2007).
- 481 33. Kennedy, P. J. *et al.* Gut memories: towards a cognitive neurobiology of
482 irritable bowel syndrome. *Neurosci. Biobehav. Rev.* **36**, 310–40 (2012).
- 483 34. Burokas, A. *et al.* Targeting the Microbiota-Gut-Brain Axis: Prebiotics Have
484 Anxiolytic and Antidepressant-like Effects and Reverse the Impact of Chronic
485 Stress in Mice. *Biol. Psychiatry* **82**, 472–487 (2017).
- 486 35. Savaignac, H. M., Kiely, B., Dinan, T. G. & Cryan, J. F. Bifidobacteria exert
487 strain-specific effects on stress-related behavior and physiology in BALB/c
488 mice. *Neurogastroenterol. Motil.* **26**, 1615–27 (2014).
- 489 36. Yang, C. *et al.* Bifidobacterium in the gut microbiota confer resilience to chronic
490 social defeat stress in mice. *Sci. Rep.* **7**, 45942 (2017).
- 491 37. Pirbaglou, M. *et al.* Probiotic supplementation can positively affect anxiety and
492 depressive symptoms: a systematic review of randomized controlled trials.
493 *Nutrition Research* (2016). doi:10.1016/j.nutres.2016.06.009
- 494 38. Huang, R., Wang, K. & Hu, J. Effect of probiotics on depression: A systematic
495 review and meta-analysis of randomized controlled trials. *Nutrients* (2016).
496 doi:10.3390/nu8080483
- 497 39. Ng, Q. X., Peters, C., Ho, C. Y. X., Lim, D. Y. & Yeo, W.-S. A meta-analysis of

- 498 the use of probiotics to alleviate depressive symptoms. *J. Affect. Disord.*
499 (2018). doi:10.1016/j.jad.2017.11.063
- 500 40. Willner, P. Validity, reliability and utility of the chronic mild stress model of
501 depression: a 10-year review and evaluation. *Psychopharmacology (Berl)*. **134**,
502 319–29 (1997).
- 503 41. Willner, P. Chronic mild stress (CMS) revisited: consistency and behavioural-
504 neurobiological concordance in the effects of CMS. *Neuropsychobiology* **52**,
505 90–110 (2005).
- 506 42. Nollet, M., Guisquet, A.-M. Le & Belzung, C. Models of Depression:
507 Unpredictable Chronic Mild Stress in Mice. *Curr. Protoc. Pharmacol.* **61**,
508 5.65.1-5.65.17 (2013).
- 509 43. Monteiro, S. *et al.* An efficient chronic unpredictable stress protocol to induce
510 stress-related responses in C57BL/6 mice. *Front. psychiatry* **6**, 6 (2015).
- 511 44. Hill, M. N. *et al.* The therapeutic potential of the endocannabinoid system for
512 the development of a novel class of antidepressants. *Trends Pharmacol. Sci.*
513 **30**, 484–93 (2009).
- 514 45. Lutz, B. Endocannabinoid signals in the control of emotion. *Curr. Opin.*
515 *Pharmacol.* **9**, 46–52 (2009).
- 516 46. Aguado, T. *et al.* The endocannabinoid system drives neural progenitor
517 proliferation. *FASEB J.* **19**, 1704–6 (2005).
- 518 47. Aguado, T. *et al.* The CB1 cannabinoid receptor mediates excitotoxicity-
519 induced neural progenitor proliferation and neurogenesis. *J. Biol. Chem.* **282**,
520 23892–8 (2007).
- 521 48. Jin, K. *et al.* Defective adult neurogenesis in CB1 cannabinoid receptor
522 knockout mice. *Mol. Pharmacol.* **66**, 204–8 (2004).
- 523 49. Dócs, K. *et al.* The Ratio of 2-AG to Its Isomer 1-AG as an Intrinsic Fine Tuning
524 Mechanism of CB1 Receptor Activation. *Front. Cell. Neurosci.* (2017).
525 doi:10.3389/fncel.2017.00039
- 526 50. Jefferies, H. B. *et al.* Rapamycin suppresses 5'TOP mRNA translation through
527 inhibition of p70s6k. *EMBO J.* **16**, 3693–704 (1997).
- 528 51. Proud, C. G. Signalling to translation: how signal transduction pathways control
529 the protein synthetic machinery. *Biochem. J.* **403**, 217–34 (2007).
- 530 52. Long, J. Z. *et al.* Selective blockade of 2-arachidonoylglycerol hydrolysis
531 produces cannabinoid behavioral effects. *Nat. Chem. Biol.* **5**, 37–44 (2009).

- 532 53. Pan, B. *et al.* Blockade of 2-Arachidonoylglycerol Hydrolysis by Selective
533 Monoacylglycerol Lipase Inhibitor 4-Nitrophenyl 4-(Dibenzo[d][1,3]dioxol-5-
534 yl(hydroxy)methyl)piperidine-1-carboxylate (JZL184) Enhances Retrograde
535 Endocannabinoid Signaling. *J. Pharmacol. Exp. Ther.* **331**, 591–597 (2009).
- 536 54. Tam, J. *et al.* Peripheral CB1 cannabinoid receptor blockade improves
537 cardiometabolic risk in mouse models of obesity. *J. Clin. Invest.* **120**, 2953–66
538 (2010).
- 539 55. Anacker, C. *et al.* Hippocampal neurogenesis confers stress resilience by
540 inhibiting the ventral dentate gyrus. *Nature* (2018). doi:10.1038/s41586-018-
541 0262-4
- 542 56. Galley, J. D. *et al.* Exposure to a social stressor disrupts the community
543 structure of the colonic mucosa-associated microbiota. *BMC Microbiol.* **14**, 189
544 (2014).
- 545 57. Jašarević, E., Rodgers, A. B. & Bale, T. L. A novel role for maternal stress and
546 microbial transmission in early life programming and neurodevelopment.
547 *Neurobiol. Stress* **1**, 81–88 (2015).
- 548 58. Marin, I. A. *et al.* Microbiota alteration is associated with the development of
549 stress-induced despair behavior. *Sci. Rep.* **7**, 43859 (2017).
- 550 59. Aizawa, E. *et al.* Possible association of Bifidobacterium and Lactobacillus in
551 the gut microbiota of patients with major depressive disorder. *J. Affect. Disord.*
552 **202**, 254–7 (2016).
- 553 60. Salaj, R. *et al.* The effects of two Lactobacillus plantarum strains on rat lipid
554 metabolism receiving a high fat diet. *ScientificWorldJournal.* **2013**, 135142
555 (2013).
- 556 61. Wu, Y., Zhang, Q., Ren, Y. & Ruan, Z. Effect of probiotic Lactobacillus on lipid
557 profile: A systematic review and meta-analysis of randomized, controlled trials.
558 *PLoS One* **12**, e0178868 (2017).
- 559 62. Schwarzer, M. *et al.* Lactobacillus plantarum strain maintains growth of infant
560 mice during chronic undernutrition. *Science (80-.).* **351**, 854–857 (2016).
- 561 63. Liu, Y.-W. *et al.* Psychotropic effects of Lactobacillus plantarum PS128 in early
562 life-stressed and naïve adult mice. *Brain Res.* **1631**, 1–12 (2016).
- 563 64. Mazure, C. M. Life Stressors as Risk Factors in Depression. *Clin. Psychol. Sci.*
564 *Pract.* **5**, 291–313 (1998).
- 565 65. Overstreet, D. H. Modeling depression in animal models. *Methods Mol. Biol.*

- 566 **829**, 125–44 (2012).
- 567 66. Moreira, F. A. & Crippa, J. A. S. The psychiatric side-effects of rimonabant.
568 *Rev. Bras. Psiquiatr.* **31**, 145–53 (2009).
- 569 67. Monteleone, P. *et al.* Investigation of CNR1 and FAAH endocannabinoid gene
570 polymorphisms in bipolar disorder and major depression. *Pharmacol. Res.* **61**,
571 400–4 (2010).
- 572 68. Denson, T. F. & Earleywine, M. Decreased depression in marijuana users.
573 *Addict. Behav.* **31**, 738–742 (2006).
- 574 69. Jiang, W. *et al.* Cannabinoids promote embryonic and adult hippocampus
575 neurogenesis and produce anxiolytic- and antidepressant-like effects. *J. Clin.*
576 *Invest.* **115**, 3104–16 (2005).
- 577 70. Zhong, P. *et al.* Monoacylglycerol lipase inhibition blocks chronic stress-
578 induced depressive-like behaviors via activation of mTOR signaling.
579 *Neuropsychopharmacology* **39**, 1763–76 (2014).
- 580 71. Hill, M. N. *et al.* Downregulation of endocannabinoid signaling in the
581 hippocampus following chronic unpredictable stress.
582 *Neuropsychopharmacology* **30**, 508–15 (2005).
- 583 72. Wang, W. *et al.* Deficiency in endocannabinoid signaling in the nucleus
584 accumbens induced by chronic unpredictable stress.
585 *Neuropsychopharmacology* **35**, 2249–61 (2010).
- 586 73. Cravatt, B. F. *et al.* Molecular characterization of an enzyme that degrades
587 neuromodulatory fatty-acid amides. *Nature* **384**, 83–7 (1996).
- 588 74. Blankman, J. L., Simon, G. M. & Cravatt, B. F. A comprehensive profile of brain
589 enzymes that hydrolyze the endocannabinoid 2-arachidonoylglycerol. *Chem.*
590 *Biol.* **14**, 1347–56 (2007).
- 591 75. McLaughlin, R. J., Hill, M. N., Morrish, A. C. & Gorzalka, B. B. Local
592 enhancement of cannabinoid CB1 receptor signalling in the dorsal
593 hippocampus elicits an antidepressant-like effect. *Behav. Pharmacol.* **18**, 431–
594 8 (2007).
- 595 76. Duric, V. *et al.* A negative regulator of MAP kinase causes depressive
596 behavior. *Nat. Med.* **16**, 1328–32 (2010).
- 597 77. Jernigan, C. S. *et al.* The mTOR signaling pathway in the prefrontal cortex is
598 compromised in major depressive disorder. *Prog. Neuropsychopharmacol.*
599 *Biol. Psychiatry* **35**, 1774–9 (2011).

- 600 78. Hill, M. N. & Gorzalka, B. B. Impairments in Endocannabinoid Signaling and
601 Depressive Illness. *JAMA* **301**, 1165 (2009).
- 602 79. Hill, M. N., Miller, G. E., Ho, W.-S. V, Gorzalka, B. B. & Hillard, C. J. Serum
603 endocannabinoid content is altered in females with depressive disorders: a
604 preliminary report. *Pharmacopsychiatry* **41**, 48–53 (2008).
- 605 80. Yi, B. *et al.* Reductions in circulating endocannabinoid 2-arachidonoylglycerol
606 levels in healthy human subjects exposed to chronic stressors. *Prog.*
607 *Neuropsychopharmacol. Biol. Psychiatry* **67**, 92–7 (2016).
- 608 81. Rueda, D., Navarro, B., Martínez-Serrano, A., Guzmán, M. & Galve-Roperh, I.
609 The Endocannabinoid Anandamide Inhibits Neuronal Progenitor Cell
610 Differentiation through Attenuation of the Rap1/B-Raf/ERK Pathway. *J. Biol.*
611 *Chem.* **277**, 46645–46650 (2002).
- 612 82. Puighermanal, E. *et al.* Cannabinoid modulation of hippocampal long-term
613 memory is mediated by mTOR signaling. *Nat. Neurosci.* **12**, 1152–8 (2009).
- 614 83. Prenderville, J. A., Kelly, Á. M. & Downer, E. J. The role of cannabinoids in
615 adult neurogenesis. *Br. J. Pharmacol.* **172**, 3950–3963 (2015).
- 616 84. Cani, P. D. *et al.* Endocannabinoids - at the crossroads between the gut
617 microbiota and host metabolism. *Nat. Rev. Endocrinol.* **12**, 133–43 (2016).
- 618 85. Muccioli, G. G. *et al.* The endocannabinoid system links gut microbiota to
619 adipogenesis. *Mol. Syst. Biol.* **6**, 392 (2010).
- 620 86. Everard, A. *et al.* Cross-talk between *Akkermansia muciniphila* and intestinal
621 epithelium controls diet-induced obesity. *Proc. Natl. Acad. Sci.* (2013).
622 doi:10.1073/pnas.1219451110
- 623 87. Guida, F. *et al.* Antibiotic-induced microbiota perturbation causes gut
624 endocannabinoidome changes, hippocampal neuroglial reorganization and
625 depression in mice. *Brain. Behav. Immun.* (2018).
626 doi:10.1016/j.bbi.2017.09.001
- 627 88. Bailey, M. T. *et al.* Exposure to a social stressor alters the structure of the
628 intestinal microbiota: implications for stressor-induced immunomodulation.
629 *Brain. Behav. Immun.* **25**, 397–407 (2011).
- 630 89. Jašarević, E., Howerton, C. L., Howard, C. D. & Bale, T. L. Alterations in the
631 Vaginal Microbiome by Maternal Stress Are Associated With Metabolic
632 Reprogramming of the Offspring Gut and Brain. *Endocrinology* **156**, 3265–
633 3276 (2015).

- 634 90. De Palma, G. *et al.* Microbiota and host determinants of behavioural phenotype
635 in maternally separated mice. *Nat. Commun.* **6**, 7735 (2015).
- 636 91. Zheng, P. *et al.* Gut microbiome remodeling induces depressive-like behaviors
637 through a pathway mediated by the host's metabolism. *Mol. Psychiatry* **21**,
638 786–796 (2016).
- 639 92. Möhle, L. *et al.* Ly6Chi Monocytes Provide a Link between Antibiotic-Induced
640 Changes in Gut Microbiota and Adult Hippocampal Neurogenesis. *Cell Rep.*
641 **15**, 1945–1956 (2016).
- 642 93. Sawada, N. *et al.* Regulation by commensal bacteria of neurogenesis in the
643 subventricular zone of adult mouse brain. *Biochem. Biophys. Res. Commun.*
644 **498**, 824–829 (2018).
- 645 94. Dinan, T. G. & Cryan, J. F. Melancholic microbes: a link between gut
646 microbiota and depression? *Neurogastroenterol. Motil.* **25**, 713–9 (2013).
- 647 95. Foster, J. A. & McVey Neufeld, K.-A. Gut-brain axis: how the microbiome
648 influences anxiety and depression. *Trends Neurosci.* **36**, 305–12 (2013).
- 649 96. Sarkar, A. *et al.* Psychobiotics and the Manipulation of Bacteria–Gut–Brain
650 Signals. *Trends Neurosci.* **39**, 763–781 (2016).
- 651 97. Rao, A. V. *et al.* A randomized, double-blind, placebo-controlled pilot study of a
652 probiotic in emotional symptoms of chronic fatigue syndrome. *Gut Pathog.* **1**, 6
653 (2009).
- 654 98. Slykerman, R. F. *et al.* Effect of Lactobacillus rhamnosus HN001 in Pregnancy
655 on Postpartum Symptoms of Depression and Anxiety: A Randomised Double-
656 blind Placebo-controlled Trial. *EBioMedicine* **24**, 159–165 (2017).
- 657 99. Akkasheh, G. *et al.* Clinical and metabolic response to probiotic administration
658 in patients with major depressive disorder: A randomized, double-blind,
659 placebo-controlled trial. *Nutrition* **32**, 315–20 (2016).
- 660 100. Bambling, M., Edwards, S. C., Hall, S. & Vitetta, L. A combination of probiotics
661 and magnesium orotate attenuate depression in a small SSRI resistant cohort:
662 an intestinal anti-inflammatory response is suggested. *Inflammopharmacology*
663 **25**, 271–274 (2017).
- 664 101. Lew, L.-C. *et al.* Probiotic Lactobacillus plantarum P8 alleviated stress and
665 anxiety while enhancing memory and cognition in stressed adults: A
666 randomised, double-blind, placebo-controlled study. *Clin. Nutr.* (2018).
667 doi:10.1016/J.CLNU.2018.09.010

- 668 102. Lafourcade, M. *et al.* Nutritional omega-3 deficiency abolishes
669 endocannabinoid-mediated neuronal functions. *Nat. Neurosci.* **14**, 345–50
670 (2011).
- 671 103. Vancassel, S. *et al.* n-3 polyunsaturated fatty acid supplementation reverses
672 stress-induced modifications on brain monoamine levels in mice. *J. Lipid Res.*
673 **49**, 340–8 (2008).
- 674 104. Falcinelli, S. *et al.* Lactobacillus rhamnosus lowers zebrafish lipid content by
675 changing gut microbiota and host transcription of genes involved in lipid
676 metabolism. *Sci. Rep.* **5**, 9336 (2015).
- 677 105. Semova, I. *et al.* Microbiota regulate intestinal absorption and metabolism of
678 fatty acids in the zebrafish. *Cell Host Microbe* **12**, 277–88 (2012).
- 679 106. Chiu, C.-H., Lu, T.-Y., Tseng, Y.-Y. & Pan, T.-M. The effects of Lactobacillus-
680 fermented milk on lipid metabolism in hamsters fed on high-cholesterol diet.
681 *Appl. Microbiol. Biotechnol.* **71**, 238–45 (2006).
- 682 107. Kishino, S. *et al.* Polyunsaturated fatty acid saturation by gut lactic acid
683 bacteria affecting host lipid composition. *Proc. Natl. Acad. Sci. U. S. A.* **110**,
684 17808–13 (2013).
- 685 108. Bao, Y. *et al.* Effect of *Lactobacillus plantarum* P-8 on lipid metabolism in
686 hyperlipidemic rat model. *Eur. J. Lipid Sci. Technol.* **114**, 1230–1236 (2012).
- 687 109. Xie, N. *et al.* Effects of two Lactobacillus strains on lipid metabolism and
688 intestinal microflora in rats fed a high-cholesterol diet. *BMC Complement.*
689 *Altern. Med.* **11**, 53 (2011).
- 690

691 **MATERIALS AND METHODS**

692
693
694 **Mice.** Adult male C57BL/6J mice (8-10 weeks old) were purchased from Janvier
695 laboratories (St Berthevin, France) and maintained under specific-pathogen free (SPF)
696 conditions at the Institut Pasteur animal care facility. Germ-free C57BL/6J mice were
697 generated at the Gnotobiology Platform of the Institut Pasteur and routinely monitored
698 for sterility. Mice were provided with food and water *ad libitum* and housed under a
699 strict 12 h light-dark cycle. All animal experiments were approved by the committee on
700 animal experimentation of the Institut Pasteur and by the French Ministry of Research.

701
702 **Fecal Microbiota Transplantation (FMT) Protocol.** Recipient mice were given a
703 combination of vancomycin (0.5 g/l), ampicillin (1 g/l), streptomycin (5 g/L), colistin (1
704 g/l), and metronidazole (0.5 g/l) in their drinking water for 6 consecutive days. All
705 antibiotics were obtained from Sigma Aldrich (St Quentin Fallavier, France). Twenty-
706 four hours later, animals were colonized via two rounds of oral gavage with microbiota,
707 separated 3 days apart, and kept in separate sterile isolators. Donor microbiota was
708 acquired from pooled fecal samples from 5-6 animals and resuspended in PBS.

709
710 **Unpredictable Chronic Mild Stress (UCMS) Protocol.** After one week of habituation
711 to the Institut Pasteur facility upon arrival, mice were subjected to various and repeated
712 unpredictable stressors several times a day during 8 weeks. During exposure to
713 stressors, mice of the UCMS group were housed in a separate room. The stressors
714 included altered cage bedding (recurrent change of bedding, wet bedding, no bedding),
715 cage tilting (45°), foreign odor (new cage impregnated with foreign mouse urine),
716 restraint (1h-1h30 in a clean 50 mL conical tube with pierced holes for ventilation),
717 altered light/dark cycle. On average, two stressors were administered per day. The

718 timeline of the stressor exposure is described in **Supplementary Table S1**. For
719 stressed animals, cages were changed after ‘wet bedding’ and ‘no bedding’ stressors.
720 Unstressed controls were handled only for injections, cage changes and behavioral
721 tests.

722

723 **CB1 Antagonists and JZL184 Treatment.** JZL184, rimonabant and AM6545 were
724 purchased from Cayman Chemicals (Bertin Technologies, Montigny-le-Bretonneux,
725 France). The drugs were dissolved in a vehicle containing a 1:1:18 mixture of ethanol,
726 kolliphor, and saline, and injected intra-peritoneally (i.p.) at a volume of $10 \mu\text{l}\cdot\text{g}^{-1}$
727 bodyweight every 2 days. Mice were injected with either vehicle alone, JZL184
728 (8mg/kg), rimonabant (2mg/kg), AM6545 (2mg/kg), JZL184 + rimonabant or JZL184 +
729 AM6545. The dose and treatment time of drug administration, alone or in combination,
730 were chosen based on previous studies showing that JZL184 irreversibly inhibits the
731 monoacylglycerol lipase (MAGL) and produces at least two-fold increase in 2-
732 arachidonoylglycerol (2-AG) levels in the brain at a dose of 8 mg/kg when dissolved in
733 the vehicle used in this study^{1,2}. Repeated administration of JZL184 at this low dose
734 does not induce observable CB1 receptor desensitization or functional tolerance³.

735

736 **Arachidonic Acid and Lactobacilli Complementation.** Arachidonic acid (AA) was
737 purchased from Cayman Chemicals (Bertin Technologies). Mice were fed every two
738 days through oral feeding gavage with 8 mg of AA/mouse/day. *Lactobacillus plantarum*
739 *Lp^{WJL}* was kindly provided by Pr. François Leulier (ENS, Lyon, France) and mice were
740 supplemented by oral feeding five days a week with 2×10^8 CFU diluted in 200 μl of
741 PBS. UCMS microbiota recipient mice were free-fed with only PBS as control.

742

743 **Microbial DNA Extraction and 16S Sequencing.** Total DNA was extracted from
744 feces using the FastDNA Spin kit, following the instructions of the manufacturer (MP
745 Biomedicals). DNA concentrations were determined by spectrophotometry using a
746 Nanodrop (Thermo Scientific). Microbial composition was assessed by 16S
747 metagenomic analysis, performed on an Illumina MiSeq instrument using a v3 reagent
748 kit. Libraries were prepared by following the Illumina “16S Metagenomic Sequencing
749 Library Preparation” protocol (Part # 15044223 Rev. B) with the following primers:
750 Forward- 5'-TCGTCGGCAGCGTCAGA TGTGTATAAGAGACAGCCTACGGGNGG-
751 CWGCAG-3'; Reverse- 5'-GTCTCGTGG GCTCGGAGATGTGTATAAGAGACAGGA-
752 CTACHVGGGTATCTAATCC-3'. PCR amplification targeted the V3-V4 region of the
753 16s rDNA. Following purification, a second PCR amplification was performed to
754 barcode samples with the Nextera XT Index Primers. Libraries were loaded onto a
755 MiSeq instrument and sequencing was performed to generate 2 x 300 bp paired-ends
756 reads. De-multiplexing of the sequencing samples was performed on the MiSeq and
757 individual FASTQ files recovered for analysis.

758
759 **16S Data Analysis.** Sequences were clustered into OTUs (Operational Taxonomic
760 Units) and annotated with the MASQUE pipeline
761 (<https://github.com/agozlane/masque>) as described⁴. OTU representative sequences
762 were assigned to the different taxonomic levels using RDP Seqmatch (RDP database,
763 release 11, update 1)⁵. Relative abundance of each OTU and other taxonomic levels
764 was calculated for each sample in order to consider different sampling levels across
765 multiple individuals. After trimming, numbers of sequences clustered within each OTU
766 (or other taxonomic levels) were converted to relative abundances. Statistical analyses
767 were performed with SHAMAN (shaman.c3bi.pasteur.fr) as described⁶. Briefly, the

768 normalization of OTU counts was performed at the OTU level using the DESeq2
769 normalization method. In SHAMAN, a generalized linear model (GLM) was fitted and
770 vectors of contrasts were defined to determine the significance in abundance variation
771 between sample types. The resulting *P*-values were adjusted for multiple testing
772 according to the Benjamini and Hochberg procedure⁷. Principal coordinates analysis
773 (PCoA) was performed with the *ade4* R package (v.1.7.6) using a Bray-Curtis
774 dissimilarity matrix. Further statistical analysis was conducted using Prism software
775 (GraphPad, v6, San Diego, USA).

776

777 **Gut permeability test.** This examination is based on the intestinal permeability to 4kD
778 fluorescent-dextran (Sigma-Aldrich). After 4 hours of food withdrawal, mice were orally
779 administered with FITC-dextran (0,6 g/kg body weight). After 1 hour, 200µl of blood
780 was collected in Microvette[®] tube (Sarstedt, Marnay, France). The tubes were then
781 centrifuged at 10 000g for 5 minutes, at room temperature, to extract the serum.
782 Collected sera were diluted with same volume of PBS and analyzed for FITC
783 concentration at excitation wavelength of 485 nm and the emission wavelength of 535
784 nm.

785

786 **Behavioral Assays.** Anxiety and depressive-like behaviors were assessed at time
787 points of interest. Mice were tested for light/dark box, splash test, novelty suppressed
788 feeding, tail suspension test and forced swim test, in that order. In order to limit the
789 eventual microbiota divergence once the recipient mice were removed from the
790 isolators, behavioral tests were performed within a week, with at least 24 hours
791 between each behavioral test. Order of passage between groups was randomized.
792 Anxiety-like behaviors were evaluated in the light/dark box (LDB) tests. Depressive-

793 like behaviors were evaluated in the splash test, the novelty suppressed feeding test,
794 the tail suspension test and the forced swim test.

795 ▪ *Light/Dark (L/D) Box*. The test was conducted in a 44x21x21 cm Plexiglas
796 box divided into dark and light compartments separated by an open door.
797 The light in the light compartment was set up at 300 lux. Time spent in
798 the light compartment and transitions between compartments during 10
799 min were video-tracked using EthoVision XT 5.1 software (Noldus
800 Information Technology).

801 ▪ *Splash test*. The splash test consists of squirting a 10% sucrose solution
802 on the dorsal coat of a mouse in its home cage. Because of its viscosity,
803 the sucrose solution dirties the mouse fur and animals initiate grooming
804 behavior. After applying sucrose solution, latency to grooming, frequency
805 and time spent grooming was recorded for a period of 6 minutes as an
806 index of self-care and motivational behavior. The splash test,
807 pharmacologically validated, demonstrates that UCMS decreases
808 grooming behavior, a form of motivational behavior considered to parallel
809 with some symptoms of depression such as apathetic behavior⁸⁻¹⁰.

810 ▪ *Novelty Suppressed Feeding (NSF)*. The NSF was carried out similar to
811 a published protocol⁹. Mice were deprived of food for 24h before being
812 placed in a novel environment, a white plastic box (50x50x20cm) whose
813 floor was covered with wooden bedding. A single food pellet (regular
814 chow) was placed on a piece of filter paper (10cm in diameter),
815 positioned in the center of the container that was brightly illuminated
816 (~500 lux). The mouse was placed in one corner of the box and the
817 latency to feed was measured during 10 min. Feeding was defined as

818 biting not simply sniffing or touching the food. Immediately after the test,
819 the animals were transferred into their home cage and the amount of food
820 consumed over the subsequent 5 min period were measured as a control
821 of feeding drive.

822 ▪ *Tail Suspension test.* Mice were suspended by the tail using adhesive
823 tape affixed 1cm from the origin of the tail, on a metal rod under dim light
824 conditions (~40 lux). The behavior of the animals was recorded by a
825 video camera during a 5 min period and total immobility time was
826 evaluated in a blind manner.

827 ▪ *Forced Swim test.* Mice were placed individually into plastic cylinders
828 (19cm diameter, 25cm deep) filled to a depth of 18 cm with water (23-
829 25°C) under dim light conditions (~40 lux) for 5 min. The behavior of the
830 animals was recorded by a video camera and immobility time was
831 automatically evaluated using EthoVision XT 5.1 software (Noldus
832 Information Technology).

833 In both TST and FST, mice face an uncomfortable situation that they confront by
834 attempting to move out of it, and eventually surrender to.

835 **5-Ethynyl-2'-deoxyuridine (EdU) Labeling.** The study of proliferation and
836 differentiation of neural stem cells in the dentate gyrus was performed by incorporation
837 of 5-ethynyl-2'-deoxyuridine (EdU, Click-iT EdU Imaging Kit; Molecular Probes) to
838 allow the analysis of proliferation and differentiation. Mice received four intraperitoneal
839 injections (100 mg/kg), at 2 h intervals, on a single day, 4 weeks before perfusion, for
840 the analysis of cell survival. EdU incorporation was visualized as described in the
841 immunohistochemistry section.

842
843 **Immunohistochemical Analysis.** Mice were deeply anesthetized with sodium
844 pentobarbital (i.p., 100 mg/ kg, Sanofi) and perfused transcardially with a solution
845 containing 0.9% NaCl and heparin (Sanofi-Synthelabo), followed by 4%
846 paraformaldehyde in phosphate buffer, pH 7.3. Brains were removed and postfixed by
847 incubation in the same fixative at 4°C overnight. Tissues were cryoprotected by
848 incubation in 30% sucrose in PBS for 24 h. Immunostaining was performed on 40- μ m
849 or 60- μ m thick coronal brain sections obtained with a vibrating microtome (VT1000S,
850 Leica). Nonspecific staining was blocked by 0.2% Triton, 4% bovine serum albumin
851 (Sigma-Aldrich) and 2% goat serum and free-floating slices were then incubated with
852 the following primary antibodies at 4°C overnight: rabbit anti-DCX (Abcam, ab 18723),
853 rabbit anti-Ki67 (Abcam, ab16667), mouse anti-NeuN (Millipore, MAB377). Secondary
854 antibodies (Alexa Fluor-conjugated secondary antibodies, Molecular Probes) were
855 then incubated at room temperature. DAPI (1 μ g/mL) was used as a nuclear stain. EdU
856 was visualized using the Click-iT reaction coupled to an Alexa Fluor® azide following
857 the instructions of the manufacturer (Molecular Probes).

858 **Image Acquisition and Quantification Analysis.** Immunofluorescence was analyzed
859 using an Apotome microscope (Apotome.2; Zeiss) with Zen Imaging software (Zeiss),
860 courtesy of Pr. Peduto. Quantification was performed using the Icy open source
861 platform (<http://www.icy.bioimageanalysis.org>)¹¹. The region of interest was defined as
862 the granule cell layer (GCL) of the dentate gyrus and automatic detection of Ki67⁺ and
863 DCX⁺ cells was performed using the spot detector tool. Values are expressed as the
864 mean of total Ki67⁺ or DCX⁺ cell count per mm² in six slices per animal. All imaging
865 and quantification were performed blinded to experimental conditions. For EdU
866 analysis, positive cells were manually counted in the GCL of the DG. Total number
867 was estimated by multiplying the total number of cells every sixth section by six.

868

869 **Western Blotting.** Mice were deeply anesthetized with sodium pentobarbital (i.p.100
870 mg/kg, Sanofi) and rapidly decapitated. The hippocampi were bilaterally dissected out
871 and then homogenized in 0.2 ml lysis buffer (pH 7.5) containing 20 mM Tris-acetate,
872 150mM NaCl, 50 mM NaF, 1 mM EDTA, 1% Triton-X100, 0.1% benzonase, protease
873 inhibitors and protein phosphatase inhibitors I and II (Sigma-Aldrich). After an
874 incubation of 30 min on ice and centrifugation at 10 000g for 10 min, total protein
875 concentration of the supernatant was assayed by using Bio-Rad protein assay kit (Bio-
876 Rad, Marnes-la-Coquette, France). Equal amounts of each protein sample were
877 separated on NuPAGE Bis-Tris or Tris-Acetate gels and transferred to nitrocellulose
878 or PVDF membranes, respectively. Blots were blocked in blocking buffer containing
879 5% (w/v) milk and 0.1% (v/v) Tween-20 in Tris-buffered saline (TBS-T) for 1~2 hours
880 at room temperature, and incubated overnight at 4°C with antibodies against p-mTOR
881 (S2448) (1:1000, Cell Signaling), mTOR (1:1000, Cell Signaling), p-p70S6K (T389)
882 (1:500, R&D Systems), p-rpS6 (S235/236) (1:500, R&D Systems) or GAPDH (1:1000,

883 Cell Signaling) antibodies. Blots were washed 3 times with TBS-T and then probed
884 with anti-rabbit IgG, HRP-linked antibody (1:3000, Cell Signaling) for 1 hour at room
885 temperature before being revealed using ECL Prime detection reagent (GE
886 Healthcare) and chemiluminescence reading on a luminescent image analyzer (LAS-
887 4000; Fujifilm). Immunoreactivity of Western blots was quantified by densitometry
888 using the ImageJ software (NIH, Bethesda).

889
890 **Biochemical Detection of 2-AG.** Mice were deeply anesthetized with sodium
891 pentobarbital (i.p.100 mg/ kg, Sanofi) and decapitated. The brain was immediately
892 removed, and the hippocampi were dissected out and rapidly frozen on dry ice. 2-AG
893 was extracted from the hippocampus as previously described¹². Samples were
894 weighed and placed into borosilicate glass culture tubes containing 2 ml of acetonitrile
895 with 186 pmol [²H₈] 2-AG. They were homogenized using IKA homogenizer and kept
896 overnight at -20°C to precipitate proteins and subsequently centrifuged at 1500g for 3
897 min. The supernatants were transferred to a new glass tube and evaporated to dryness
898 under N₂ gas. The samples were resuspended in 500µl of methanol to recapture any
899 lipids adhering to the glass tube and dried again under N₂ gas. Dried lipid extracts
900 were suspended in 50µl of methanol and stored at -80°C until analysis. The content of
901 2-AG was determined using isotope- dilution liquid chromatography–electrospray
902 ionization tandem mass spectrometry (LC-MS/MS)¹³.

903
904 **Metabolomics.** Blood were collected by cardiac puncture in Microvette® tubes
905 (Sarstedt, Marnay, France), from behaviorally validated adult mice. The tubes were
906 centrifuged at 10 000g for 5 minutes, at room temperature, to extract the serum. Serum
907 samples were then extracted and analyzed on GC/MS, LC/MS and LC/MS/MS

908 platforms by Metabolon, Inc (California, USA). Protein fractions were removed by serial
909 extractions with organic aqueous solvents, concentrated using a TurboVap system
910 (Zymark) and vacuum dried. For LC/MS and LC/MS/MS, samples were reconstituted
911 in acidic or basic LC-compatible solvents containing > 11 injection standards and run
912 on a Waters ACQUITY UPLC and Thermo-Finnigan LTQ mass spectrometer, with a
913 linear ion-trap front-end and a Fourier transform ion cyclotron resonance mass
914 spectrometer back-end. For GC/MS, samples were derivatized under dried nitrogen
915 using bistrimethyl-silyl-trifluoroacetamide and analyzed on a Thermo-Finnigan Trace
916 DSQ fast-scanning single-quadrupole mass spectrometer using electron impact
917 ionization. Chemical entities were identified by comparison to metabolomic library
918 entries of purified standards. Following log transformation and imputation with
919 minimum observed values for each compound, data were analyzed using two-way
920 ANOVA with contrasts.

921
922 **Statistical analysis.** Statistical analysis was performed using Prism software
923 (GraphPad, v6, San Diego, USA). Principal component analyses (PCA) and heatmaps
924 were performed using Qlucore Omics Explorer (Qlucore). Data are plotted in the
925 figures as mean \pm SEM. Differences between two groups were assessed using Mann-
926 Whitney test. Differences among three or more groups were assessed using one-way
927 ANOVA with Tukey's. Significant differences are indicated in the figures by * $p < 0.05$,
928 ** $p < 0.01$, *** $p < 0.001$, **** $p < 0.0001$. Notable near-significant differences ($0.05 < p$
929 < 0.1) are indicated in the figures. Notable non-significant (and non-near significant)
930 differences are indicated in the figures by "n.s".

931
932 **Data availability.** The data that support the findings of this study are available from
933 the corresponding author upon request.

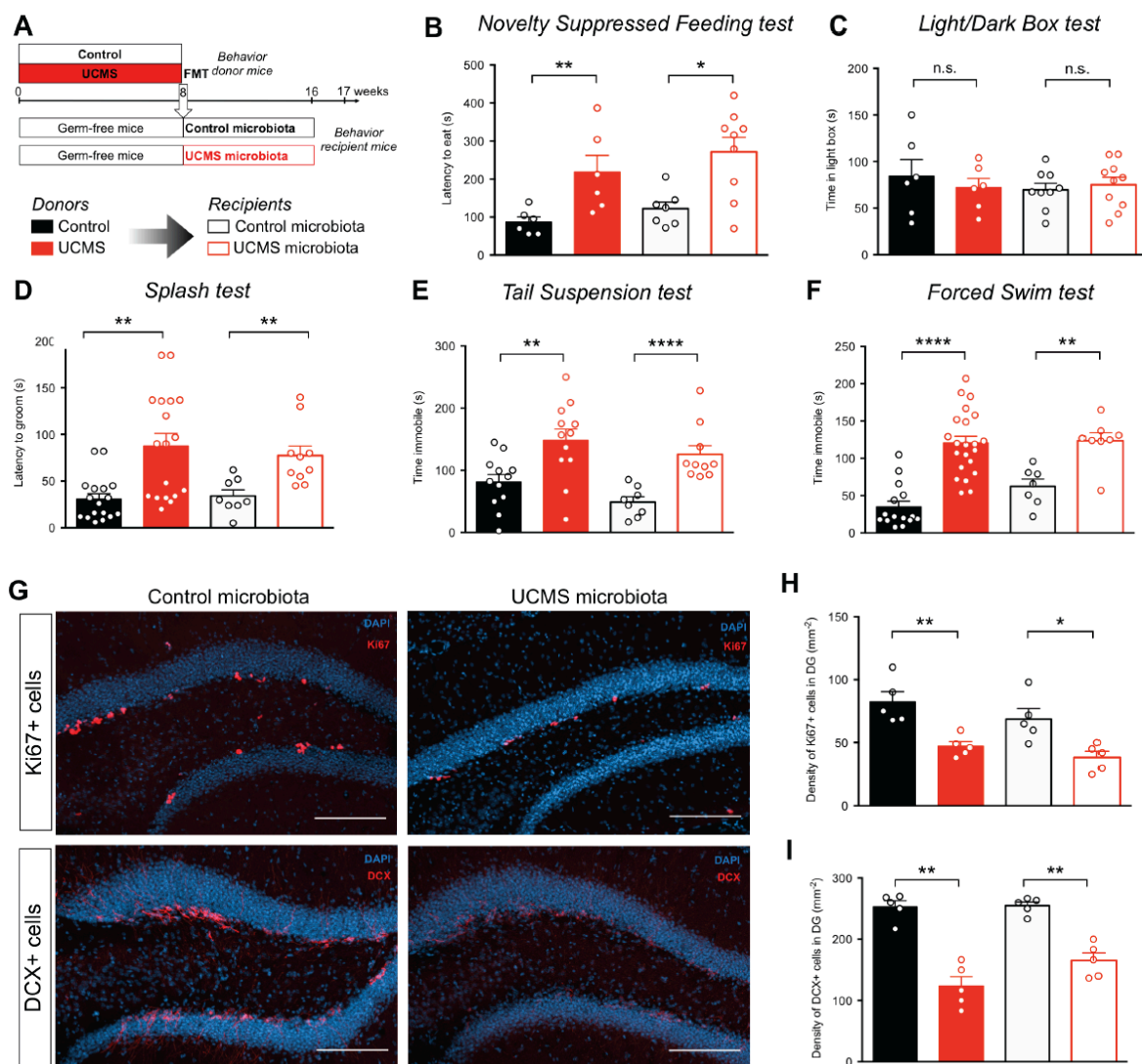
934 **REFERENCES for METHODS**

- 935 1. Long, J. Z. *et al.* Selective blockade of 2-arachidonoylglycerol hydrolysis produces
936 cannabinoid behavioral effects. *Nat. Chem. Biol.* **5**, 37–44 (2009).
- 937 2. Zhong, P. *et al.* Monoacylglycerol lipase inhibition blocks chronic stress-induced
938 depressive-like behaviors via activation of mTOR signaling.
939 *Neuropsychopharmacology* **39**, 1763–76 (2014).
- 940 3. Kinsey, S. G. *et al.* Repeated low-dose administration of the monoacylglycerol
941 lipase inhibitor JZL184 retains cannabinoid receptor type 1-mediated
942 antinociceptive and gastroprotective effects. *J. Pharmacol. Exp. Ther.* **345**, 492–
943 501 (2013).
- 944 4. Quereda, J. J. *et al.* Bacteriocin from epidemic *Listeria* strains alters the host
945 intestinal microbiota to favor infection. *Proc. Natl. Acad. Sci. U. S. A.* **113**, 5706–
946 11 (2016).
- 947 5. Cole, J. R. *et al.* The Ribosomal Database Project: improved alignments and new
948 tools for rRNA analysis. *Nucleic Acids Res.* **37**, D141-5 (2009).
- 949 6. Dickson, L. B. *et al.* Carryover effects of larval exposure to different environmental
950 bacteria drive adult trait variation in a mosquito vector. *Sci. Adv.* **3**, e1700585
951 (2017).
- 952 7. Benjamini, Y. & Hochberg, Y. Controlling the False Discovery Rate: A Practical
953 and Powerful Approach to Multiple Testing. *Journal of the Royal Statistical Society.*
954 *Series B (Methodological)* **57**, 289–300 (1995).
- 955 8. Ducottet, C., Aubert, A. & Belzung, C. Susceptibility to subchronic unpredictable
956 stress is related to individual reactivity to threat stimuli in mice. *Behav. Brain Res.*
957 **155**, 291–9 (2004).
- 958 9. Nollet, M., Guisquet, A.-M. Le & Belzung, C. Models of Depression: Unpredictable
959 Chronic Mild Stress in Mice. *Curr. Protoc. Pharmacol.* **61**, 5.65.1-5.65.17 (2013).
- 960 10. Santarelli, L. *et al.* Requirement of Hippocampal Neurogenesis for the Behavioral
961 Effects of Antidepressants. *Science (80)*. **301**, 805–809 (2003).

- 962 11. de Chaumont, F. *et al.* Icy: an open bioimage informatics platform for extended
963 reproducible research. *Nat. Methods* **9**, 690-6 (2012).
- 964 12. Wang, W. *et al.* Deficiency in endocannabinoid signaling in the nucleus accumbens
965 induced by chronic unpredictable stress. *Neuropsychopharmacology* **35**, 2249–61
966 (2010).
- 967 13. Patel, S., Rademacher, D. J. & Hillard, C. J. Differential regulation of the
968 endocannabinoids anandamide and 2-arachidonylglycerol within the limbic
969 forebrain by dopamine receptor activity. *J. Pharmacol. Exp. Ther.* **306**, 880–8
970 (2003).

971 **FIGURE LEGENDS**

Figure 1

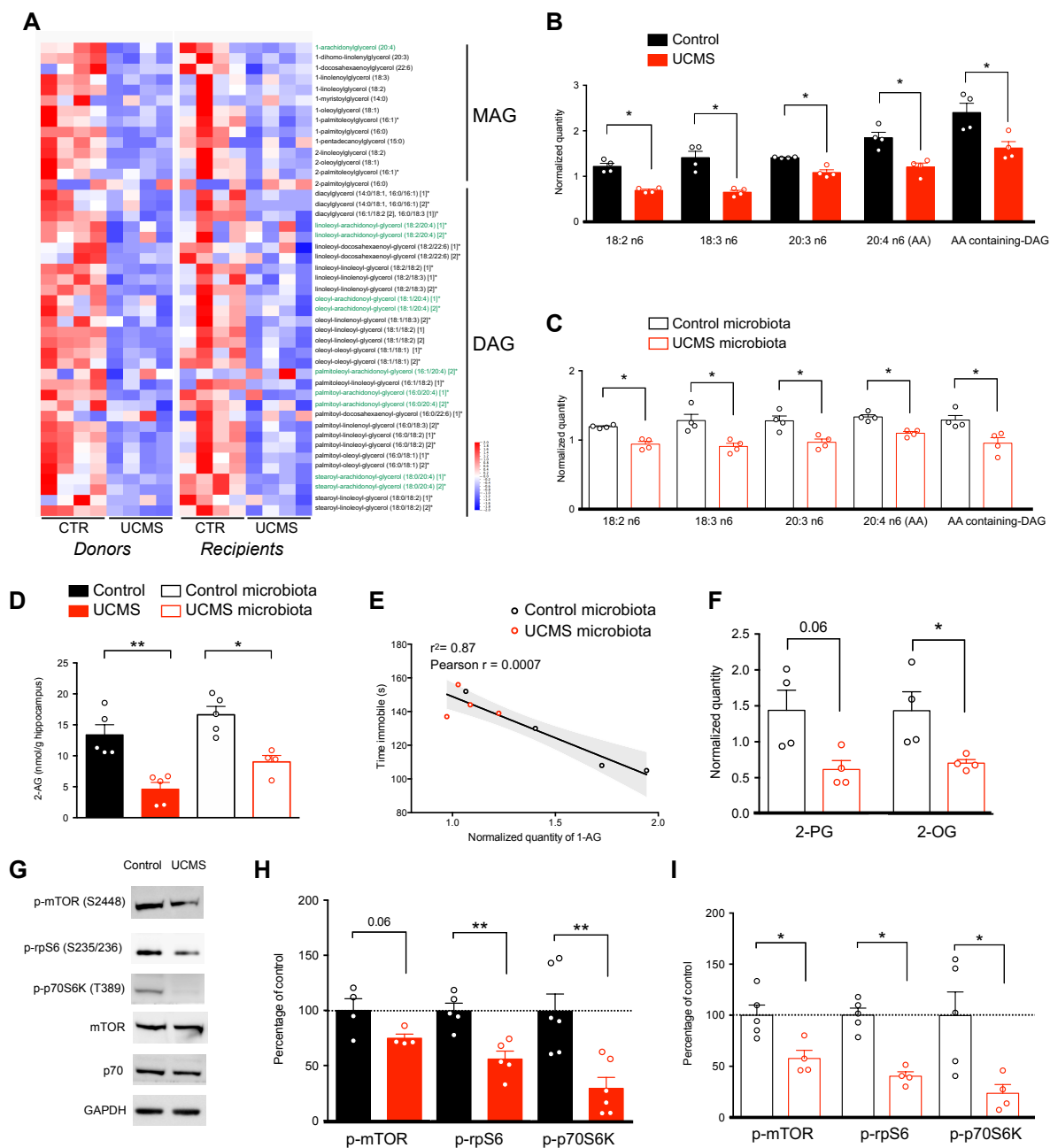


972

973 **Figure 1. Microbiota from UCMS Mice Transfers Depressive-like Behaviors and**
 974 **Reduces Adult Hippocampal Neurogenesis.** **A**, Experimental timeline of Fecal
 975 Microbiota Transplantation (FMT) from Control and UCMS mice, respectively 'Control
 976 microbiota' and 'UCMS microbiota', to germ-free recipient mice. **B-F**, Control mice

977 (black bars), or mice subjected to UCMS (red bars), and mice recipient of the microbiota
978 from Control (open black bars) or UCMS mice (open red bars), underwent different
979 behavioral tests. **B**, Latency to eat in a novel environment in the Novelty Suppressed
980 Feeding test for Control mice ($n = 6$), UCMS mice ($n = 6$), Control microbiota-recipient
981 mice ($n = 7$) and UCMS microbiota-recipient mice ($n = 9$). (Control vs UCMS, $P =$
982 0.0087; Control microbiota- vs UCMS microbiota-recipient mice, $P = 0.0229$); **C**, Time
983 spent in the light box in the Light/Dark Box test for Control mice ($n = 6$), UCMS mice (n
984 = 6), Control microbiota-recipient mice ($n = 9$) and UCMS microbiota-recipient mice (n
985 = 10). (Control vs UCMS, $P = 0.6991$; Control microbiota- vs UCMS microbiota-recipient
986 mice, $P = 0.6038$); **D**, Latency to groom in the Splash test for Control mice ($n = 17$),
987 UCMS mice ($n = 18$), Control microbiota-recipient mice ($n = 8$) and UCMS microbiota-
988 recipient mice ($n = 10$). (Control vs UCMS, $P = 0.0004$; Control microbiota- vs UCMS
989 microbiota-recipient mice, $P = 0.0012$); **E**, Time spent immobile in the Tail Suspension
990 Test for Control mice ($n = 10$), UCMS mice ($n = 10$), Control microbiota-recipient mice
991 ($n = 8$) and UCMS microbiota-recipient mice ($n = 10$). (Control vs UCMS, $P = 0.0043$;
992 Control microbiota- vs UCMS microbiota-recipient mice, $P < 0.0001$); **F**, Time spent
993 immobile in the Forced Swim Test for Control mice ($n = 15$), UCMS mice ($n = 22$),
994 Control microbiota-recipient mice ($n = 7$) and UCMS microbiota-recipient mice ($n = 8$).
995 (Control vs UCMS, $P < 0.0001$; Control microbiota- vs UCMS microbiota-recipient mice,
996 $P = 0.0037$). **G**, Representative images of Ki67 staining (top) and DCX staining (bottom)
997 in the DG of the hippocampus, counterstained with DAPI (blue), in Control microbiota-
998 recipient mice (left) and UCMS microbiota-recipient mice (right). **H**, Quantitative
999 evaluation of the density of Ki67⁺ cells in the dentate gyrus (DG) of the hippocampus
1000 for Control mice ($n = 5$), UCMS mice ($n = 5$), Control microbiota-recipient mice ($n = 5$)
1001 and UCMS microbiota-recipient mice ($n = 5$). (Control vs UCMS, $P = 0.0079$; Control
1002 microbiota- vs UCMS microbiota-recipient mice, $P = 0.0159$). Scale bar: 100 μ m. **I**,
1003 Quantitative evaluation of the density of DCX⁺ cells in the DG of the hippocampus for
1004 Control mice ($n = 5$), UCMS mice ($n = 5$), Control microbiota-recipient mice ($n = 5$) and
1005 UCMS microbiota-recipient mice ($n = 5$). (Control vs UCMS, $P = 0.0079$; Control
1006 microbiota- vs UCMS microbiota-recipient mice, $P = 0.0079$) For (**B** to **I**) Data are
1007 represented as mean \pm s.e.m. Statistical significance was calculated using the Mann
1008 Whitney test ($*P < 0.05$, $**P < 0.01$, $***P < 0.001$, $****P < 0.0001$).

Figure 2

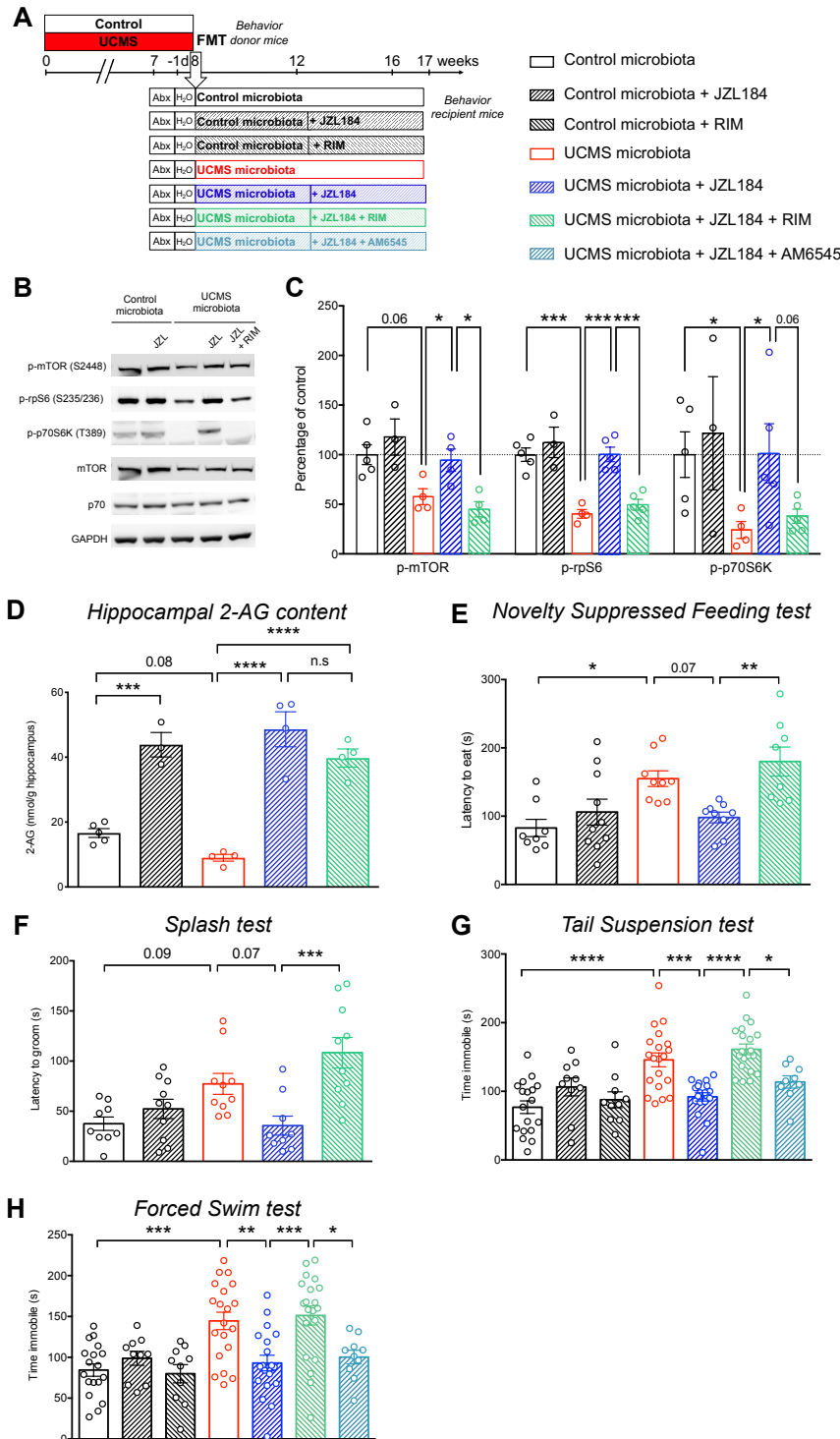


1009

1010 **Figure 2. Microbiota from UCMS mice alters fatty acid metabolism and**
 1011 **hippocampal eCB system.** **A**, Heatmap of normalized serum levels of
 1012 Monoacylglycerols (MAG) and Diacylglycerols (DAG) in donor ($n = 4$ /group) and
 1013 recipient mice ($n = 4$ /group) (z-scored). Arachidonic acid-containing MAG and DAG
 1014 are highlighted in green. **B-C**, Normalized levels of fatty acid in the synthesis pathway

1015 of arachidonic acid (AA) and AA-containing DAG in donor mice ($n = 4$; **B**) and in
1016 recipient mice ($n = 4$, **C**). For **B** and **C**, data are represented as mean \pm s.e.m.
1017 Statistical significance was calculated using the Mann Whitney test (*, $P = 0.0286$). **D**,
1018 Concentration of 2-AG in the hippocampus of donor ($n = 5$ /group) and recipient mice
1019 ($n = 5$ /group) was determined by targeted LC-MS (Control vs UCMS, $P = 0.0079$;
1020 Control microbiota- vs UCMS microbiota-recipient mice, $P = 0.0159$). **E**, Correlation
1021 between serum quantity of 1-AG and time spent immobile in the tail suspension test
1022 (TST) in recipient mice ($n = 4$ /group). Correlation was calculated using Pearson
1023 correlation factor r ($r = 0.0007$). **F**, Normalized quantity of the two minor
1024 endocannabinoids 2-PG and 2-OG in the serum of recipient mice ($n = 4$ /group). (2-PG,
1025 $P = 0.0571$; 2-OG, $P = 0.0286$). **G**, Representative western blots for p-mTOR (S2448),
1026 p-rpS6 (S235/236), p-p70S6K (T389), mTOR, p70 and GAPDH in hippocampal protein
1027 extracts from donor mice. **H-I**, Quantification of the phosphorylation of mTOR, rpS6
1028 and p70S6K in protein extracts from the hippocampus of Control and UCMS donor
1029 mice (p-mTOR, $n = 4$, $P = 0.0571$; p-rpS6, $n = 5$, $P = 0.0079$; p-p70S6K, $n = 6$, $P =$
1030 0.0087 ; **E**) and Control microbiota- ($n = 5$) and UCMS microbiota-recipient mice ($n =$
1031 4) (p-mTOR, $P = 0.0317$; p-rpS6, $P = 0.0159$; p-p70S6K, $P = 0.0317$; **F**). For **B**, **C**, **D**,
1032 **F**, **H** and **I**, data are represented as mean \pm s.e.m. Statistical significance was
1033 calculated using the Mann Whitney test (* $P < 0.05$, ** $P < 0.01$).

Figure 3



1034

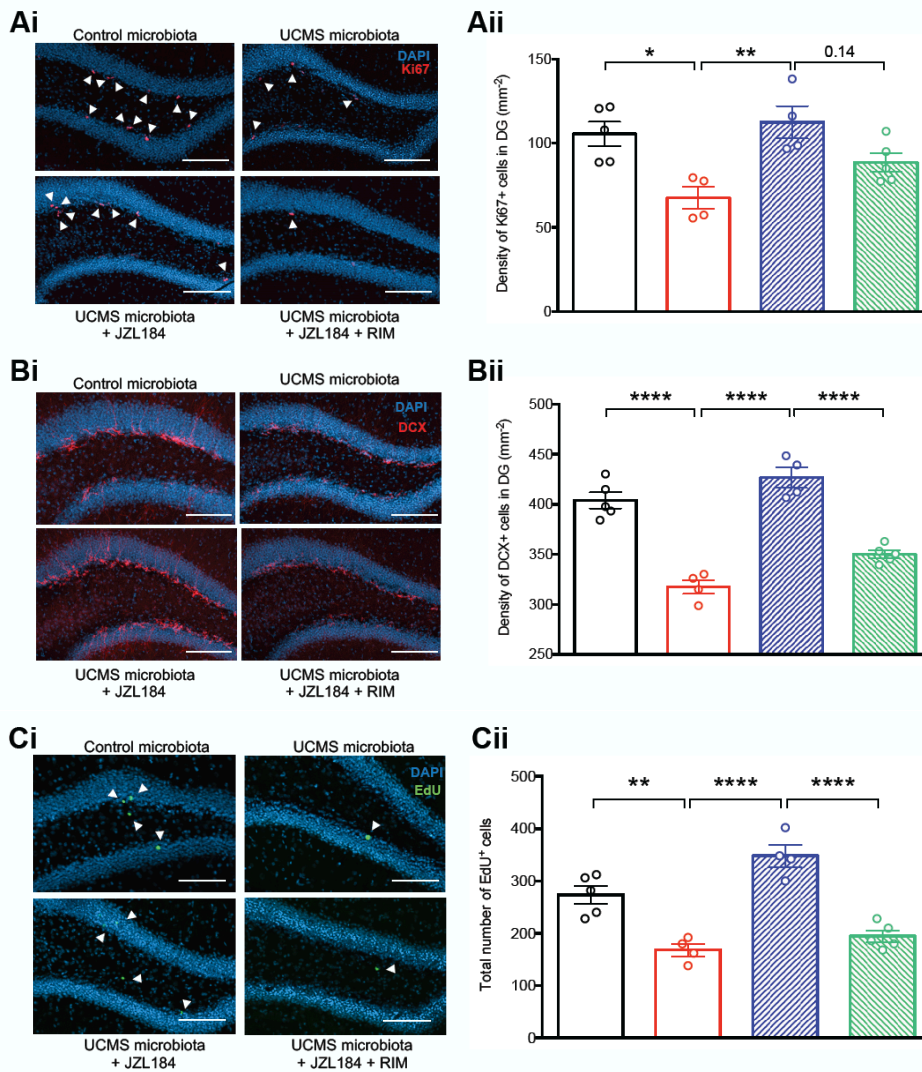
1035 **Figure 3 Restoration of the eCB pathway normalizes behavior in recipient mice.**

1036 **A**, Experimental timeline of JZL184, rimonabant (RIM) and AM6545 treatment in
 1037 recipient mice. Mice were injected intra-peritoneally every 2 days, with either vehicle
 1038 alone, JZL184 (8mg/kg), rimonabant (2mg/kg), AM6545 (2mg/kg), JZL184 +
 1039 rimonabant or JZL184 + AM6545. The treatment started 4 weeks after FMT and lasted

1040 for 5 weeks, until sacrifice. **B**, Representative western blots for p-mTOR (S2448), p-
1041 rpS6 (S235/236), p-p70S6K (T389), mTOR, p70 and GAPDH in hippocampal protein
1042 extracts from recipient mice upon treatment with JZL184 or rimonabant. **C**,
1043 Quantification of the phosphorylation of mTOR, rpS6 and p70S6K in hippocampal
1044 protein extracts from Control microbiota-recipient mice ($n = 5$), Control microbiota-
1045 recipient mice treated with JZL184 ($n = 3$), UCMS microbiota-recipient mice ($n = 4$),
1046 UCMS microbiota-recipient mice treated with JZL184 ($n = 5$, except for p-mTOR with n
1047 = 4), UCMS microbiota-recipient mice treated with JZL184 and rimonabant ($n = 5$,
1048 except for p-mTOR with $n = 4$). Control microbiota and UCMS microbiota groups are
1049 the same as in figure 2I. (p-mTOR: Control vs UCMS-recipient mice, $P = 0.0317$;
1050 UCMS-recipient mice vs UCMS-recipient mice + JZL184, $P = 0.0571$; UCMS-recipient
1051 mice + JZL184 vs UCMS-recipient mice + JZL184 + RIM, $P = 0.0286$; p-rpS6: Control
1052 vs UCMS-recipient mice, $P = 0.0159$; UCMS-recipient mice vs UCMS-recipient mice +
1053 JZL184, $P = 0.0159$; UCMS-recipient mice + JZL184 vs UCMS-recipient mice + JZL184
1054 + RIM, $P = 0.0079$; p-p70S6K: Control vs UCMS-recipient mice, $P = 0.0317$; UCMS-
1055 recipient mice vs UCMS-recipient mice + JZL184, $P = 0.0317$; UCMS-recipient mice +
1056 JZL184 vs UCMS-recipient mice + JZL184 + RIM, $P = 0.0556$). **D**, Concentration of 2-
1057 AG in the hippocampus of Control microbiota-recipient mice ($n = 5$), Control microbiota-
1058 recipient mice treated with JZL184 ($n = 3$), UCMS microbiota-recipient mice ($n = 4$),
1059 UCMS microbiota-recipient mice treated with JZL184 ($n = 4$) and UCMS microbiota-
1060 recipient mice treated with JZL184 and rimonabant ($n = 4$), as determined by targeted
1061 LC-MS. Control microbiota and UCMS microbiota groups are the same as in figure 2D.
1062 (Control microbiota-recipient vs Control microbiota-recipient mice + JZL184, $P =$
1063 0.0002; Control microbiota-recipient vs UCMS microbiota-recipient mice, $P = 0.0872$;
1064 UCMS microbiota-recipient vs UCMS microbiota-recipient mice + JZL184, $P < 0.0001$;
1065 UCMS microbiota-recipient vs UCMS microbiota-recipient mice + JZL184 + RIM, $P <$
1066 0.0001; UCMS microbiota-recipient + JZL184 vs UCMS microbiota-recipient mice +
1067 JZL184 + RIM, $P = 0.3037$). **E**, Latency to eat in a novel environment in the Novelty
1068 Suppressed Feeding test for Control microbiota-recipient mice ($n = 8$), Control
1069 microbiota-recipient mice treated with JZL184 ($n = 10$), UCMS microbiota-recipient
1070 mice ($n = 9$), UCMS microbiota-recipient mice treated with JZL184 ($n = 9$), UCMS
1071 microbiota-recipient mice treated with JZL184 and rimonabant ($n = 8$). (Control
1072 microbiota- vs UCMS microbiota-recipient mice, $P = 0.0179$; UCMS microbiota-
1073 recipient mice vs UCMS microbiota-recipient mice + JZL184, $P = 0.0796$; UCMS

1074 microbiota-recipient mice + JZL184 vs UCMS microbiota-recipient mice + JZL184 +
1075 RIM, $P = 0.0054$). **F**, Latency to groom in the splash test for Control microbiota-recipient
1076 mice ($n = 9$), Control microbiota-recipient mice treated with JZL184 ($n = 10$), UCMS
1077 microbiota-recipient mice ($n = 10$), UCMS microbiota-recipient mice treated with
1078 JZL184 ($n = 9$), UCMS microbiota-recipient mice treated with JZL184 and rimonabant
1079 ($n = 10$). (Control microbiota- vs UCMS microbiota-recipient mice, $P = 0.0946$; UCMS
1080 microbiota-recipient mice vs UCMS microbiota-recipient mice + JZL184, $P = 0.0721$;
1081 UCMS microbiota-recipient mice + JZL184 vs UCMS microbiota-recipient mice +
1082 JZL184 + RIM, $P = 0.0003$). **G**, Time spent immobile in the Tail Suspension test for
1083 Control microbiota-recipient mice ($n = 18$), Control microbiota-recipient mice treated
1084 with JZL184 ($n = 10$), Control microbiota-recipient mice treated with rimonabant ($n =$
1085 10), UCMS microbiota-recipient mice ($n = 20$), UCMS microbiota-recipient mice treated
1086 with JZL184 ($n = 19$), UCMS microbiota-recipient mice treated with JZL184 and
1087 rimonabant ($n = 20$) and UCMS microbiota-recipient mice treated with JZL184 and
1088 AM6545 ($n = 9$). (Control microbiota- vs UCMS microbiota-recipient mice, $P < 0.0001$;
1089 UCMS microbiota-recipient mice vs UCMS microbiota-recipient mice + JZL184, $P =$
1090 0.0002 ; UCMS microbiota-recipient mice + JZL184 vs UCMS microbiota-recipient mice
1091 + JZL184 + RIM, $P < 0.0001$; UCMS microbiota-recipient mice + JZL184 + RIM vs
1092 UCMS microbiota-recipient mice + JZL184 + AM6545, $P = 0.0266$). **H**, Time spent
1093 immobile in the Forced Swim test for Control microbiota-recipient mice ($n = 18$), Control
1094 microbiota-recipient mice treated with JZL184 ($n = 10$), Control microbiota-recipient
1095 mice treated with rimonabant ($n = 10$), UCMS microbiota-recipient mice ($n = 20$), UCMS
1096 microbiota-recipient mice treated with JZL184 ($n = 19$), UCMS microbiota-recipient
1097 mice treated with JZL184 and rimonabant ($n = 20$) and UCMS microbiota-recipient mice
1098 treated with JZL184 and AM6545 ($n = 10$). (Control microbiota- vs UCMS microbiota-
1099 recipient mice, $P = 0.0003$; UCMS microbiota-recipient mice vs UCMS microbiota-
1100 recipient mice + JZL184, $P = 0.0028$; UCMS microbiota-recipient mice + JZL184 vs
1101 UCMS microbiota-recipient mice + JZL184 + RIM, $P = 0.0004$; UCMS microbiota-
1102 recipient mice + JZL184 + RIM vs UCMS microbiota-recipient mice + JZL184 +
1103 AM6545, $P = 0.0276$). Data are represented as mean \pm s.e.m. For **C** to **H**, statistical
1104 significance was calculated using One-way ANOVA with Tukey's multiple comparisons
1105 test (* $P < 0.05$, ** $P < 0.01$, *** $P < 0.001$, **** $P < 0.0001$).

Figure 4



1106

1107 **Figure 4. Restoration of the eCB pathway normalizes hippocampal neurogenesis.**

1108 **Ai**, Representative images of Ki67 staining (red) in the DG of the hippocampus,

1109 counterstained with DAPI (blue). **Aii**, Quantitative evaluation of the density of Ki67+ cells

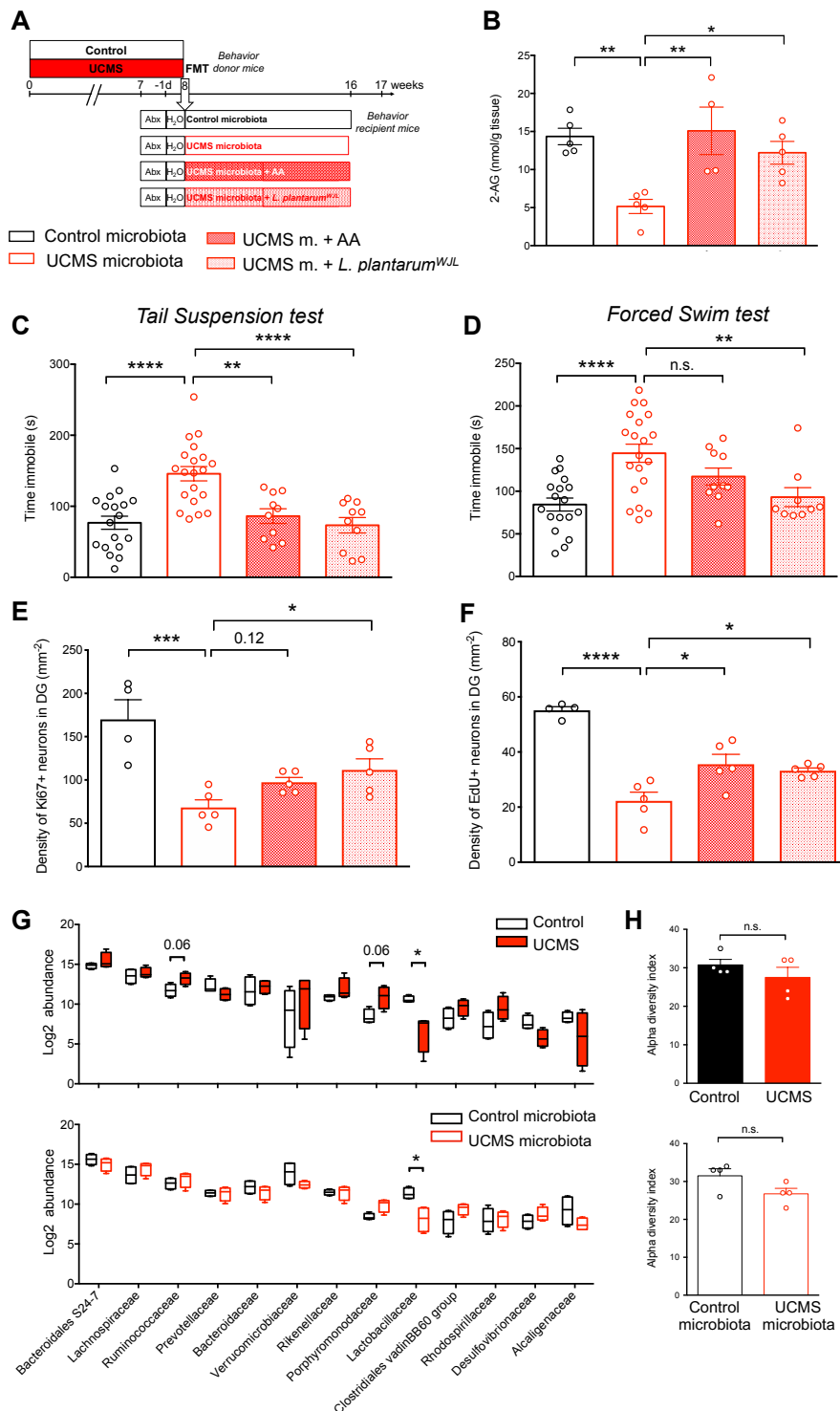
1110 for Control microbiota-recipient mice ($n = 5$), UCMS microbiota-recipient mice ($n = 4$),

1111 UCMS microbiota-recipient mice treated with JZL184 ($n = 4$), UCMS microbiota-

1112 recipient mice treated with JZL184 and rimonabant ($n = 5$). (Control microbiota- vs
1113 UCMS microbiota-recipient mice, $P = 0.0111$; UCMS microbiota-recipient mice vs
1114 UCMS microbiota-recipient mice + JZL184, $P = 0.0048$; UCMS microbiota-recipient
1115 mice + JZL184 vs UCMS microbiota-recipient mice + JZL184 + RIM, $P = 0.1402$). **Bi**,
1116 Representative images of DCX staining (red) in the DG of the hippocampus,
1117 counterstained with DAPI (blue). **Bii**, Quantitative evaluation of the density of DCX⁺
1118 cells for Control microbiota-recipient mice ($n = 5$), UCMS microbiota-recipient mice (n
1119 = 4), UCMS microbiota-recipient mice treated with JZL184 ($n = 4$), UCMS microbiota-
1120 recipient mice treated with JZL184 and rimonabant ($n = 5$). (Control microbiota- vs
1121 UCMS microbiota-recipient mice, $P < 0.0001$; UCMS microbiota-recipient mice vs
1122 UCMS microbiota-recipient mice + JZL184, $P < 0.0001$; UCMS microbiota-recipient
1123 mice + JZL184 vs UCMS microbiota-recipient mice + JZL184 + RIM, $P < 0.0001$). **Ci**,
1124 Representative images of EdU staining (green) in the DG of the hippocampus,
1125 counterstained with DAPI (blue). **Cii**, Quantitative evaluation of total number of EdU⁺
1126 cells for Control microbiota-recipient mice ($n = 5$), UCMS microbiota-recipient mice (n
1127 = 4), UCMS microbiota-recipient mice treated with JZL184 ($n = 4$), UCMS microbiota-
1128 recipient mice treated with JZL184 and rimonabant ($n = 5$). (Control microbiota- vs
1129 UCMS microbiota-recipient mice, $P = 0.0014$; UCMS microbiota-recipient mice vs
1130 UCMS microbiota-recipient mice + JZL184, $P < 0.0001$; UCMS microbiota-recipient
1131 mice + JZL184 vs UCMS microbiota-recipient mice + JZL184 + RIM, $P < 0.0001$). Scale
1132 bars: 100 μ m. Data are represented as mean \pm s.e.m. Statistical significance was
1133 calculated using One-way ANOVA with Tukey's multiple comparisons test ($*P < 0.05$,
1134 $** P < 0.01$, $**** P < 0.0001$).

1135

Figure 5



1136

1137 **Figure 5. Arachidonic acid or *Lactobacillus plantarum*^{WJL} complementations are**
 1138 **sufficient to normalize hippocampal 2-AG levels, adult neurogenesis and**
 1139 **behavior. A,** Experimental timeline of arachidonic acid (AA) and *L. plantarum*
 1140 treatment in recipient mice. Mice were fed every two days through oral gavage with
 1141 8 mg of AA/mouse/day. Mice were supplemented by oral feeding five days a week with

1142 2×10^8 CFU diluted in 200 μ l of PBS. UCMS microbiota recipient mice were oral-fed
1143 with PBS as control. **B**, Concentration of 2-AG in the hippocampus for Control
1144 microbiota ($n = 5$), UCMS microbiota ($n = 5$), UCMS microbiota complemented with AA
1145 ($n = 4$) and UCMS microbiota complemented with Lp^{WJL} ($n = 5$), as determined by
1146 targeted LC-MS (Control microbiota- vs UCMS microbiota-recipient mice, $P = 0.0062$;
1147 UCMS microbiota-recipient mice vs UCMS microbiota-recipient mice + AA, $P = 0.0053$;
1148 UCMS microbiota-recipient mice vs UCMS microbiota-recipient mice + Lp^{WJL} , $P =$
1149 0.0371). **C**, Time spent immobile in the Tail Suspension Test for Control microbiota-
1150 recipient mice ($n = 18$), UCMS microbiota-recipient mice ($n = 20$), UCMS microbiota-
1151 recipient mice complemented with AA ($n = 10$) and UCMS microbiota-recipient mice
1152 complemented with Lp^{WJL} ($n = 10$) (Control microbiota- vs UCMS microbiota-recipient
1153 mice, $P < 0.0001$; UCMS microbiota-recipient mice vs UCMS microbiota-recipient mice
1154 + AA, $P = 0.0015$; UCMS microbiota-recipient mice vs UCMS microbiota-recipient mice
1155 + Lp^{WJL} , $P < 0.0001$). **D**, Time spent immobile in the Forced Swim test for Control
1156 microbiota-recipient mice ($n = 18$), UCMS microbiota-recipient mice ($n = 20$), UCMS
1157 microbiota-recipient mice complemented with AA ($n = 10$) and UCMS microbiota-
1158 recipient mice complemented with Lp^{WJL} ($n = 9$) (Control microbiota- vs UCMS
1159 microbiota-recipient mice, $P < 0.0001$; UCMS microbiota-recipient mice vs UCMS
1160 microbiota-recipient mice + AA, $P = 0.2690$; UCMS microbiota-recipient mice vs UCMS
1161 microbiota-recipient mice + Lp^{WJL} , $P = 0.0083$). Data are represented as mean \pm s.e.m.
1162 Statistical significance was calculated using one-way ANOVA with Tukey's multiple
1163 comparisons test (** $P < 0.01$, **** $P < 0.0001$). **E**, quantitative evaluation of the density
1164 of Ki67⁺ cells for Control microbiota-recipient mice ($n = 4$), UCMS microbiota-recipient
1165 mice ($n = 5$), UCMS microbiota-recipient mice complemented with AA ($n = 5$), UCMS
1166 microbiota-recipient mice complemented with Lp^{WJL} ($n = 5$) (Control microbiota- vs
1167 UCMS microbiota-recipient mice, $P = 0.0003$; UCMS microbiota-recipient mice vs
1168 UCMS microbiota-recipient mice + AA, $P = 0.1175$; UCMS microbiota-recipient mice
1169 vs UCMS microbiota-recipient mice + Lp^{WJL} , $P = 0.0258$). **F**, Quantitative evaluation of
1170 the density of EdU⁺ cells for Control microbiota-recipient mice ($n = 4$), UCMS
1171 microbiota-recipient mice ($n = 5$), UCMS microbiota-recipient mice complemented with
1172 AA ($n = 5$), UCMS microbiota-recipient mice complemented with Lp^{WJL} ($n = 5$) (Control
1173 microbiota- vs UCMS microbiota-recipient mice, $P < 0.0001$; UCMS microbiota-
1174 recipient mice vs UCMS microbiota-recipient mice + AA, $P = 0.0113$; UCMS
1175 microbiota-recipient mice vs UCMS microbiota-recipient mice + Lp^{WJL} , $P = 0.0394$). **G**,

1176 16S rDNA of the fecal microbiota of donor mice at the end of the 8 weeks UCMS
1177 protocol ($n = 4/\text{group}$, top) or recipients mice after 8 weeks in isolators ($n = 4/\text{group}$,
1178 bottom), was sequenced and analyzed by principal Component Analysis (PCA) at the
1179 level of bacterial families for the relative abundance of bacterial families. Data are
1180 represented as boxplots. Statistical significance was calculated using Mann-Whitney
1181 test (top, *Ruminococcaceae*, $P = 0.0571$; *Porphyromonadaceae*, $P = 0.0571$;
1182 *Lactobacillaceae*, $P = 0.0286$; bottom, *Lactobacillaceae*, $P = 0.0286$). **H**, Alpha
1183 diversity for donors ($P = 0.6857$, top) and recipients ($P = 0.2286$). Data are represented
1184 as mean \pm s.e.m. Statistical significance was calculated using Mann-Whitney test. For
1185 **B** to **F**, data are represented as mean \pm s.e.m. Statistical significance was calculated
1186 using one-way ANOVA with Tukey's multiple comparisons test (* $P < 0.05$, *** $P <$
1187 0.0005 , **** $P < 0.0001$).